ECOLE POLYTECHNIQUE FEDERALE DE LAUSANNE
SCHOOL OF LIFE SCIENCES

Master's project in Bioengineering and Biotechnology

Development of high content image-based cell viability assays

by

Julien Mena

Under the direction of Dr. Gerardo Turcatti, Senior Scientist
In the Biomolecular Screening Facility EPFL

External Expert: Dr. Cameron Scott, PhD

LAUSANNE, EPFL 2010

Abstract

Aim and applications

- Optimize fluorescence-based cellular assays for getting insights about mechanisms leading to cell death.
- Informative high content assays development with the aim to implement them in order to obtain preliminary toxicity information of compounds.
- Toxicity profiling of chemicals or biologicals used in screening, in particular hits behavior relative to the characterization of cell viability.

Methods

Different fluorescent probes for cell viability were tested and optimized in HeLa cells by varying parameters of staining, controls and incubation times. Automated fluorescence microscopy was used to image cells in 96-well plates and automated image analysis provided tool for quantification of the response to the different assays. Image quality was estimated in each condition and ability to discriminate between positive and negative populations was statistically determined after image segmentation and features extraction.

Results

Live/dead assay using calcein-AM and ethidium homodimer-1 showed significant difference in signal between living and dead cells but high variability was observed within the same population. Apoptosis probes FLICA and annexin V conjugate were tested on cells treated with staurosporine. FLICA staining gave low signal-to-background ratio and apoptotic population was not significantly discernible. Living, early apoptotic and necrotic/late apoptotic cells populations were segregated using annexin V assay. Autophagy detection using LC3B immunostaining was observable in cells treated with chloroquine. Developed image analysis method reliably segmented autophagosomes in autophagic cells but failed with dead cells. Assays were tested on a set of toxic compounds and results showed differences with information found on these substances.

Conclusion

Fluorescent probes are a powerful tool to assess cell death mechanism in high content screening assay as they can report multiple biological activities at the same time. As information in this type of assay are gathered at a single cell level, high variability is expected and must be reduced as possible to successfully characterize the phenotypes encountered and reach screening requirements.

Keywords: High content screening; High throughput screening; Fluorescence-based cellular assays; Cell death; Toxicity studies

I. List of figures

II. List of tables

III. List of abbreviations

Abbreviation	Meaning
ABC transporter	ATP-binding cassette transporter
ATG gene	Autophagy-related gene
BD	Becton Dickinson
BSA	Bovine serum albumin
BSF	Biomolecular screening facility
Calcein-AM	Calcein-Acetoxymethyl
CCD	Charge-coupled device
DAPI	4',6-diamidino-2-phenylindole
DMSO	Dimethyl sulfoxide
DNA	Deoxyribonucleic acid
EDTA	Ethylenediaminetetraacetic acid
EthD-1	Ethidium homodimer-1
EthOH	Ethanol
FAM	Carboxyfluorescein
FBS	Fetal bovine serum
FLICA	Fluorescent inhibitor of caspases
FMK	Fluoromethyl ketone
FRET	Fluorescence resonance energy transfer
GBA	Gambogic acid
GFP	Green fluorescent protein
HCA	High content analysis
HCS	High content screening
HeLa cell	Henrietta Lacks cell
HTS	High throughput screening
IC_{50}	Half maximal inhibitory concentration
LC3 A/B/C	Microtubule-associated protein 1 light chain 3 A/B/C
NA	Numerical aperture
PBS	Phosphate buffer saline
PS	Phosphatidylserine
RB nXn	Rolling ball of size n (image processing algorithm)
ROI	Region of interest
RT	Room temperature (about 22°C)
SD	Standard deviation
T4O	Terpinen-4-ol
VPA	Valproïc acid
xyFOV	Field of view in the xy plane

IV. Table of content

1. Introduction

1.1. High content image-based screening

Drug discovery is the process by which a molecule is found to have a biological effect against a disease in an organism. During the past years, scientists have developed automated equipments that allow performing a consequent number of parallel experiments in a time that can never be achieved by manual manipulations. This automation process and the fact that multiple compounds are tested at the same time are called high throughput screening (HTS). During a screen, the activity of each compound is reported by an assay that quantitatively determines the potency of the molecule on the target effect. The assay read out can take various forms like fluorescence quantification or colorimetric measurements. Typically, the following steps can describe the HTS process applied to drug discovery:

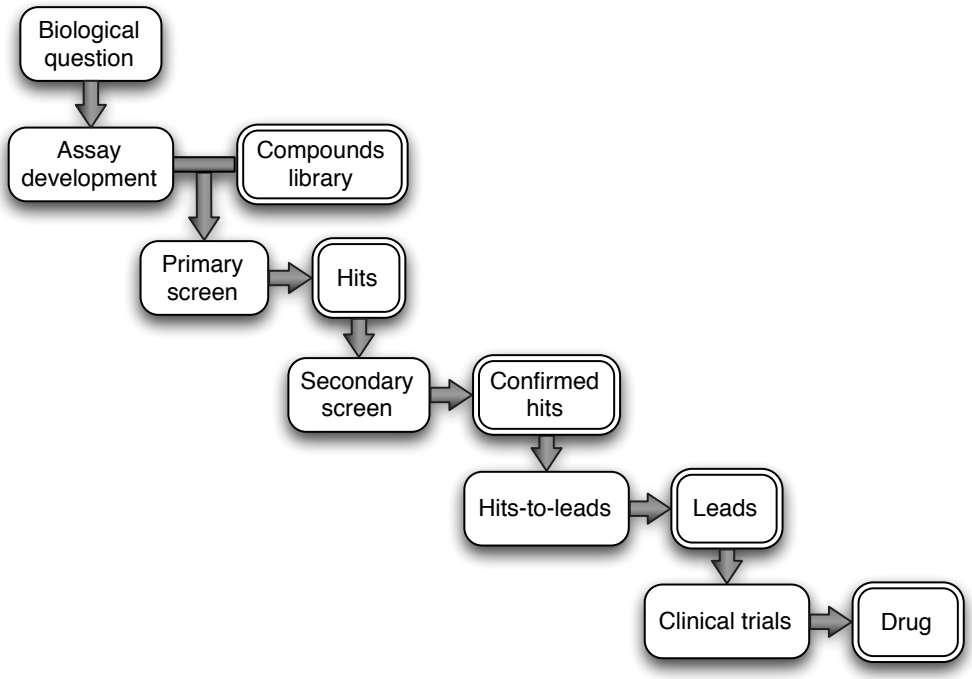

Figure 1. **Drug discovery process using high throughput screening.**
From a biological question, a target or a mechanism is identified and allows developing an assay that relates the phenomenon. A compounds library is then chosen to be tested on the target effect and the primary screen is performed. Compounds that showed activity in the primary screen are called hits. These molecules are further tested and validated in a secondary screen. The resulting hits are then studied in detail for features like structure-activity relationship, toxicity or pharmacokinetics. The molecules are optimized and some will become leads that will eventually be tested in clinical trials and become a drug candidate.

When the read out of a high throughput screening assay is images, the process is commonly named high content screening (HCS). This new generation of screening method introduced in the mid-1990s[1] is emerging and becoming a powerful tool for drug discovery as well as for other life science research applications. In fact, the recent technological advancements like automated microscopy, new fluorophores discovery or increased computational power have enhanced the capability for acquiring and analyzing images.[2] High content screening is more often performed in secondary screen or hit-to-lead studies, the drug discovery step where

compounds that showed significant activity during previous screen are re-tested and validated. The workflow of a high content screen is described in Figure 2.

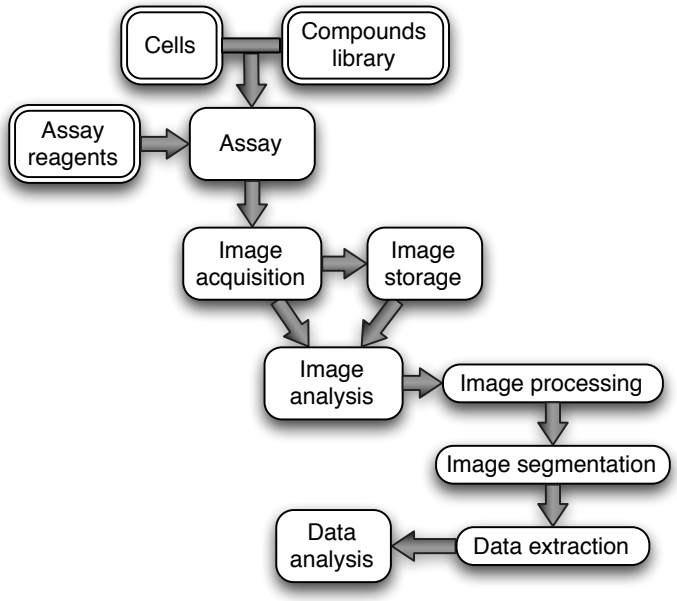

Figure 2. **High content screening workflow.**

Cells and compounds are incubated together and the assay is performed using the appropriate reagents. The images of cell phenotypes are then acquired and stored. After eventual image processing, images are analyzed to extract data for segmented regions of interest (ROI) that reflect the response of each cell to the compound. Data analysis determines which compounds had significant effect by comparing their response to the controls.

Compared to conventional high throughput screen, image-based screening has several advantages and drawbacks. One of the major advantages is that high content screening assays can easily be multiplexed, meaning that signals from different events can be obtained from a single experiment. In fact, it is common in high content assays to use several probes that report different information for each single cell tested. One can then for instance get a measure of cell viability and a response to a specific assay like protein expression level within the same experiment. It has been shown that multiplexing application was the second most relevant application for high content screens, just after signaling pathway analysis.[3]

Another feature of image-based assays is that the information is gathered at the cell level unlike most of conventional end point read-outs that get a measure at a cell population level. Due to the complexity of living systems, each cell, even clonal, produces slightly to highly different response for a same experimental condition and thus, variability in high content assays tend to be higher than in assays that measure overall response of a cell population.[4] However, the observed response reflects better the variability of the biological system and then gives more information on how cells behave individually. Generally, high content screening assay are considered to produce lower rate of false-positive and false-negative than conventional assay.[5]

Imaging gives also the possibility to perform testing at sub-cellular resolution like protein relocation or organelles quantification that are difficult to test by other means.

Regarding data storage and handling, high content screening raises more difficulties than conventional screens. For instance, an end-point fluorescent assay typically gives one data (fluorescence emission) for each well but a high content assay can provide several images per well. In terms of computing data mass, this means that the ratio between conventional screens and high content screen is the range of order of 1:4000 (1 octet for single digit and about 2

Mo per image with a minimum of two images). Thus, high content screens easily generated a data mass in the Teraoctet range, implying more storage cost and also more difficulties for data handling. Image compression is an option to reduce data mass but it is important not to loose information that could compromise image analysis.
A possibility to get a data mass similar to conventional screen is to perform image acquisition, analysis and segmentation at the same time and store only the value of the extracted features of segmentation (i.e. dye intensity or nucleus area) while discarding the images. Nevertheless, this method removes the possibility to re-analyze images to get other data or inspect images by eyes which could be interesting to confirm hits and reduce false positive rate. Another reason to keep images is that a more powerful or specific software can be released, giving more possibilities to extract data.
Despite all advancements in microscopy automation, image-based screens are much more time-consuming than other screens. In fact, taking images automatically is a complex process, especially regarding finding the focus position. A common method to find quite precisely the focus point is image-based autofocus. A stack of different z-position images are acquired and analyzed by image processing algorithm that determine which image of the stack is the most in-focus. This unavoidable step of imaging considerably increases the time to take images because several images have to be acquired and analyzed.
In summary, high content screening opens the way for assaying cell biology features that are difficult to test with other assays. The obtained data tend to be closer from the real variability of the biological system.

1.2. Cell viability

Cell viability is a key topic in the drug discovery process because the toxicity of compounds has to be intensely tested to be able to become a drug candidate. In fact, the earlier in the discovery process the compound is found to have harmful effect, the faster a go/no go decision can be taken and precious time and investments can be saved. More, it might be meaningful to get a maximum of information on the toxicity source so that promising hits can be well characterized. Hit-to-lead optimization could also take advantage of this information for following up drug candidates.
The death of mammalian cells has been classified in three distinct modes: apoptosis, necrosis and autophagy-associated death. These classifications have been set thanks to the different morphological changes and biochemical pathways that lead to the cell death. Programmed cell death is the process by which a cell that receives endogenous or exogenous signal, triggers a genetically control pathway that will lead to its death. Apoptosis is the most known programmed cell death although autophagy-associated is also genetically predetermined. It has been shown that the cell death pathways are linked and some signaling molecules have been proposed as molecular switches between the different modes induced cell death.[6,7,8]

1.2.1. Apoptosis

The term apoptosis has been introduced for the first time in 1842 by Carl Vogt, a German scientist emigrated in Switzerland, while he was working in Neuchâtel on the development of tadpole (aquatic larval stage of amphibian).[9] Since then, apoptosis has been highly studied especially in the 1990th for its importance in cancer, tissue renewal and many other relevant biological fields.
Two major pathways can initiate apoptosis: the death receptor pathway and the mitochondrial pathway. The death receptors are trans-membrane proteins that have affinity for death inducing signaling molecules such as members of tumor necrosis factor family. When bound to a ligand, these receptors initiate cell death by formation of a multi-protein death-inducing

complex that will activate caspase 8, central proteolytic mediator of apoptosis. The balance between pro- and anti-apoptotic members of the Bcl-2 protein family regulates mitochondrial activation of apoptosis.[10] In fact, some proteins of this family (BAX and BAK) tend to initiate apoptosis by increasing permeability of mitochondrial membranes and inducing the release of cytochrome *c* while other like *Bcl2* or *Bcl-XL* do exactly the opposite. If the balance tips in pro-apoptotic agents favor, the apoptotic process is initiated and the release of cytochrome *c* leads to the formation of apoptosomes that activate caspase 9. This pathway is typically activated when concentration of intracellular reactive oxygen species increases, DNA is damaged or the cell is deprived of growth factors.

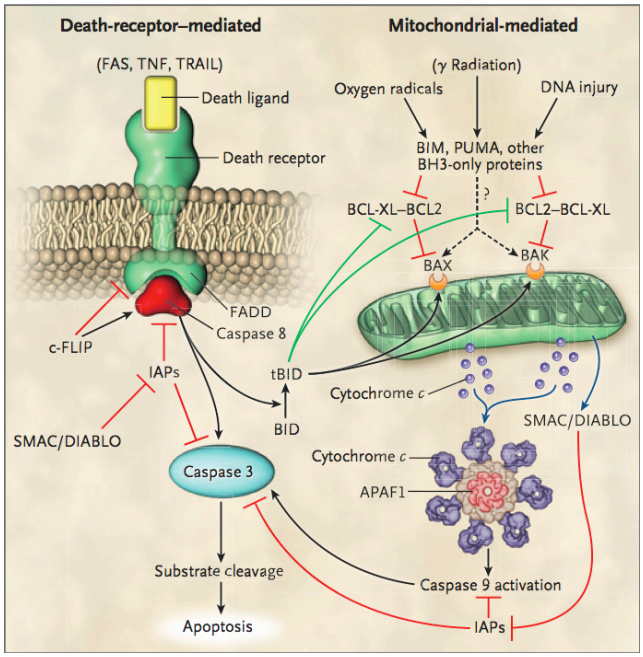

Figure 3. **Pathway of apoptosis activation.**

This figure extracted from *Cell Death* by Hotchkiss et al.[10] describes the two different pathways of activation of apoptosis.

Caspases are cysteine proteases and are central mediators and effectors of apoptosis. The activation of caspase 8 (death receptor) or caspase 9 (mitochondria) mobilize the caspases 3, 6, and 7 that will start to cleave lots of different proteins in the cell and also activate DNases. The activation of caspases causes the specific morphological changes observed in apoptosis[11] by breaking down the cellular matrix and cytoskeleton proteins.

Morphological changes	Biochemical changes
Nuclear compaction	Activation of caspases and p53
Nuclear fragmentation	Loss of mitochondrial membrane potential
Cell shrinkage	Mitochondrial membrane permeabilization
Plasma membrane blebbing	Phosphatidylserine exposure
Reduction of cellular and nuclear volume	

Table 1. **Morphological and biochemical changes due to apoptosis.**

This non-exhaustive list shows some of the changes that can be observed during apoptosis.

Other biochemical changes occur during apoptosis like translocation of phosphatidylserine. In viable cells, membrane proteins called flippases constantly maintain plasmic membrane asymmetry by inverting phosphatidylserine to the cytoplasmic side of the cell. When the cell enters the execution phase of apoptosis, phosphatidylserine is no more translocated to the inner side of cell, resulting in exposure of phosphatidylserine to the outer surface of the cell. This exposure is a signal for macrophages and phagocytes that will eliminate the dying cell.[12] This event appends after the activation of the caspases but before the breakdown of the plasmic membrane, which integrity is kept until late stage of apoptosis.

1.2.2. Autophagy-associated death

Autophagy (from Greek "phagy": to eat, "auto": oneself) is a process by which the cell generates energy and metabolites by digesting its own components. This state is triggered by a lack of nutrients and aims to make the cell survive.[10] It is reversible until a certain point if the cell receives nutrients but if it's not the case, the cell digests itself to death.
Autophagy happens in four sequential steps: induction, autophagosome formation, degradation and reuse.[13] The induction of autophagy is typically due to lack of an essential type of nutrient. In yeast, nitrogen, carbon or single amino acid starvation has been shown to induce autophagy.[14] In mammals, the autophagic process is thought to be highly regulated because nutrients consumption and repartition is an important issue for an entire organism. The depletion of all amino acids and some individual amino acid starvation induces autophagy.[15] During autophagosome formation, cell constituents such as cytoplasm components or organelles are randomly sequestered in a double-layer membrane from a not well-known origin. The resulting engulfing organelle is called autophagosome. The compositions of the inner and outer membrane of the autophagosome are different. In mammalian cells, only one component has been identified in the inner membrane.[13] This homolog of yeast Atg8 is called LC3 and is present in three isoforms all bounded to autophagosome membrane but that show distinct sub-cellular localization patterns in autophagic cell (LC3A, LC3B and LC3C).[16] Other genes, called ATG (AuTophaGy-related) have been identified to be involved in the regulation and execution of autophagy.[17] The next step of the autophagic process is the degradation of the material enclosed in the autophagosome by lysosomal or vacuolar hydrolases. Finally, the obtained monomeric nutrients (amino acids, saccharides, etc) are released from the autophagosome after the breakdown of its membrane and reused for cell metabolism.

Morphological changes	Biochemical changes
Vacuolization of cytoplasm	LC3 localization in autophagosomes membrane
Loss of organelles	ATG complex signaling formation
Formation of autophagosomes	

Table 2. **Morphological and biochemical changes due to autophagy.**
This non-exhaustive list shows some of the changes that can be observed during autophagy.

1.2.3. Necrosis

Necrosis is described as the default pathway of death. A necrotic event is recorded when the cell is not in apoptosis or autophagy. However, necrosis shows specific morphological and biochemical changes. Although this type of death is not genetically programmed, some

modulators have been observed in the course of the events in necrosis. The sequence starts with mitochondrial swelling and release of reactive oxygen species in the cytoplasm. The increase of intracellular Ca^{2+} ions activates some proteases like calpain or cathepsin that digest key proteins of the cell. Rupture of lysosomal membrane releases other proteases and leads to cell demolition and plasma membrane rupture.[18] Compared to apoptosis and autophagy, cell membrane integrity is rapidly lost in necrosis. Some morphological and biochemical changes are listed in Table 3.

Morphological changes	Biochemical changes
Cytoplasmic swelling	Calpain and cathepsin activation
Rapid plasma membrane rupture	ATP depletion
Cytoplasmic organelles swelling	Intracellular Ca2+ increase
Moderate chromatin condensation	

Table 3. **Morphological and biochemical changes due to necrosis.**
This non-exhaustive list shows some of the changes that can be observed during necrosis.

1.3. Fluorescent probes

Fluorescence spectroscopy is a powerful approach to assess living cell mechanisms by using appropriate fluorescent molecules. These probes consist of a molecule that identifies specifically a target in a cell or a complex organism and reports about activity, location or concentration by fluorescence emission monitoring. The read-out can be done by spectrofluorometry or microscopy, which offers more possibilities as described in Chapter 1.1. The major characteristics of a fluorescent probe are: delivery, targeting, detectability and fluorescence response.[19] Delivery is the way by which the probe reaches the target e.g. a protein, ion or organelle. Generally, probes are designed to be lipophilic so they cross membranes and can have access to cytoplasmic components or intra-organelle targets. It is also possible to add a low concentration of detergent that will permeabilize the membrane and allow the probe to enter the cell. Targeting reflects the specificity of the probe for the target. To design fluorescent probes, a fluorescent tag (fluorescein, GFP) can be added to a molecule known to have interactions with the desired target. Specificity has to be well characterized so the observed response is consistent with the studied phenomenon. Detectability is related to the fluorescent attributes of the probes such as quantum yield, extinction coefficient or excitation/emission wavelengths. It includes all parameters that influence the way a probe can be detected with the instrumentation. Fluorescence response characterizes the interaction of the probes with the physiological environment. Mechanisms like FRET, quenching, pH sensitivity or fluorescence shift has to be studied as they can interfere with the response one wants to observe using the probe.
Fluorescent probes are intensively used in high content screening. A lot of applications and assay kits have been developed and this area is constantly growing. Below, some fluorescent dyes are described in particular these to assess cell viability.

1.3.1. Hoechst and DAPI

4',6-diamidino-2-phenylindole (DAPI) and Hoechst are nucleic acid stains. They principally bind to minor groove of DNA in AT-rich region and are excited by ultraviolet light with a maximum of absorbance around 350 nm.[20] They re-emit a cyan/blue light with an emission peak at 461 nm that is about 20-fold more intense than their natural fluorescence.

Both dyes can cross the cell membranes but Hoechst is more lipophilic thanks to an additional ethyl group and thus pass through the membrane more efficiently. These dyes are used to stain the nucleus of cells and can information such as cell number, nuclear shape or cell localization.

	Hoechst
Chemical structure	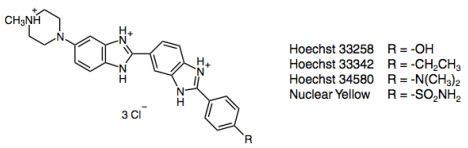
	DAPI
Chemical structure	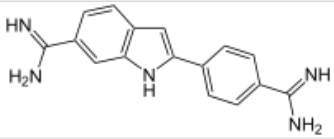
Spectra	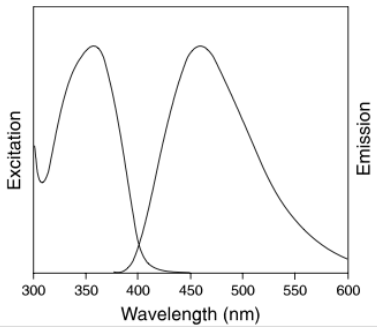
Max. absorption	358 nm
Max. emission	461 nm

1.3.2. Calcein AM

Calcein is a derivative of fluorescein broadly used to determine cell viability. In fact, the acetoxymethyl ester form (calcein AM) is non-fluorescent and crosses the cell's membrane passively. Once it has entered the cell, cytosolic esterases activity removes the ester group and the fluorescent calcein is retained within the cell. If cell's membrane is not intact, calcein is diluted in the medium and the cytosol of the cell is not fluorescent.[21] It has been shown that calcein is excluded by multidrug resistance protein (ABC transporter) and thus cannot be used for cells that express such transporters.[22]

Calcein has also been described as mitochondrial membrane potential reporter when used with cobalt ions that quenches its cytoplasmic fluorescence.[23] In summary, cells that are positive for calcein staining are considered as viable thanks to their esterase activity and plasmic membrane integrity.

	Calcein AM
Chemical structure	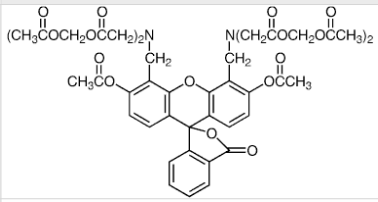
Spectra	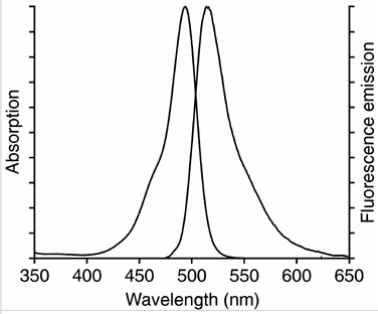
Max. absorption	495 nm
Max. emission	515 nm

1.3.3. Ethidium homodimer-1

	Ethidium homodimer-1
Chemical structure	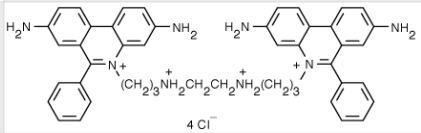
Spectra	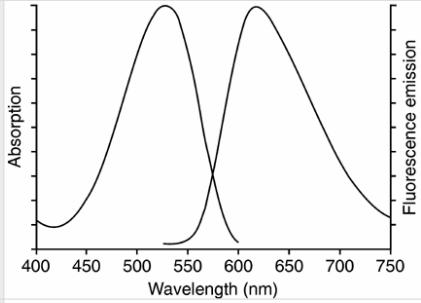
Max. absorption	528 nm
Max. emission	617 nm

Ethidium homodimer-1 (EthD-1) is a dye that has high affinity for nucleic acids. As it has low membrane permeability, it doesn't enter cell with intact membranes. Thus, only nucleus of cells with damaged membrane is stained with EthD-1 and these cells are considered as dead or dying cells. EthD-1 has 40-fold red emission fluorescence (max. at 617 nm) when bound to nucleic acids and its spectra does not overlap with green-fluorescent esterase probes as calcein AM.

EthD-1 is similar to propidium iodide but superior to ethidium bromide thanks to a binding strength to nucleic acid around 1000 times higher. This high affinity and enhanced fluorescence allow to use EthD-1 at a small concentration compared to ethidium bromide and doesn't need a wash step due to low background fluorescence.

1.3.4. FLICA

	FLICA
Chemical structure	FAM-Asp-Glu-Val-Asp-FMK Carboxyfluorescein-peptide sequence-fluoromethyl ketone
Spectra (Carboxyfluorescein)	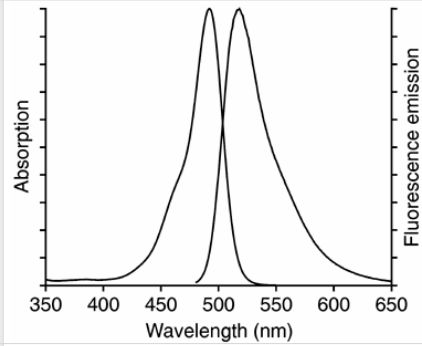
Max. absorption	488 nm
Max. emission	530 nm

FLuorescent Inhibitors of CAspases (FLICA) have been developed to test for apoptosis. As detailed in Chapter 1.2.1, caspases are effector proteases involved in apoptosis pathway. FLICA are composed of three parts: a fluoromethyl ketone (FMK) group, a short peptide sequence and a carboxyfluorescein (FAM) group and this molecule is membrane permeable. The FLICA inhibit caspases thanks to the covalent binding of FMK to a cysteine in the caspases reaction site. This interaction is possible because the short peptide sequence is specific to a caspase and several of them have been found to be recognized by different caspases. For instance, the amino acid sequence Asp-Glu-Val-Asp (DEVD) is specific for caspase 3 and 7 while Leu-Glu-Thr-Asp (LETD) has affinity for caspase 8. The FAM group is the fluorescent reporter that allows the molecule to be detected by fluorescence imaging. Thus, cells that have enough activated caspases should be stained by FLICA showing their apoptotic state.

1.3.5. Annexin V conjugate

Annexin V conjugate	
Protein structure	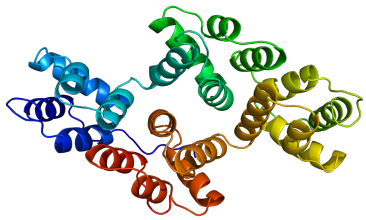
Spectra (Alexa 488)	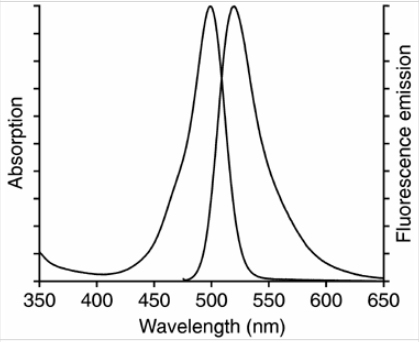
Max. absorption	488 nm
Max. emission	530 nm

Annexin V was first isolated from a fraction of human umbilical cord artery in 1985 reported by Reutelingsperger et al.[24] for its anticoagulant properties. The protein was then expressed in bacteria thanks to cDNA cloning and was found to have numerous activities such as anticoagulant, anti-phospholipase or trans-membrane channel activity.[25] However, the phospholipid binding property of annexin V is the most known. In fact, annexin V binds to phosphatidylserine (PS) in presence of Ca^{2+} and can therefore be used to detect apoptosis. As explain in Chapter 1.2.1, phosphatidylserine is translocated to the outer surface of the cell during apoptosis and acts as an elimination signal for macrophages and phagocytes. To detect apoptosis, annexin V is conjugated to a fluorophore (e.g. Alexa Fluor® 488) and added with Ca^{2+} in the supernatant of the cells to be tested. As this probe is not membrane permeable, external side of the membrane of cells that have exposed PS is stained, enlightening their apoptotic state. However if cell membrane is broken meaning that the cell is in late state apoptosis or necrosis, annexin V enters the cell and binds to cytoplasmic-oriented PS. This implies that annexin V probe should be used with proper counter-stain like propidium iodide or EthD-1 that enters only membrane-damaged cells and permits to discriminate between apoptotic and late apoptotic/necrotic cells. In summary, annexin V combined with nuclear and dead cell counter-stain allows to distinguish three populations of cells: viable cells (stained only with nuclear probe), early apoptotic cells (stained with nuclear and annexin V probes) and late state apoptotic/necrotic cells (stained with nuclear, annexin V probes and dead cell counter-stain).

1.3.6. LC3B antibody

In Chapter 1.2.2, LC3B has been described to be linked to the membrane of autophagosomes, the effectors organelles of autophagy. Antibody against LC3B can thus be used to detect autophagy using immunostaining procedure. Autophagosomes are located in the cytoplasm of autophagic cells and as antibodies cannot cross cell membrane, the use of a detergent that will permeabilize the membrane is unavoidable. The primary antibody has specific affinity for LC3B protein can then enters the cell and binds to this protein on the membrane of autophagosomes. A secondary antibody against antibody of the species in which the primary antibody has been produced, will bound to the primary antibody. This secondary antibody is conjugated with a fluorophore that can be detected by fluorescence microscopy. Cells that are in autophagic state should show small bright dots in their cytoplasm, representing the autophagosomes.

1.4. Assay development

The aim of assay development in HTS cell-based assay is to set up a measurable and reliable reporter of a biological activity. The reporter, or probe, interacts with a target mechanism that reflects the cellular activity to be evaluated and the emitted signal quantitatively defines the activity of a cell or a cell population. Once a reporter is found to significantly give a difference in signal between relevant phenotypes of cells, the assay has to be intensively optimized to reach the high-throughput screening requirements.

In HCS, probes are most of the time fluorescent molecules that can bind to a target cellular component or be modified by cellular metabolism resulting in a change of their fluorescence properties. Probes should accurately reflect the underlying biology and minimize artifacts thanks to high specificity for the target mechanism. For HCS assays, the two most important parameters to be optimized are: high signal-to-background ratio and low variability.[26] Every step of the assay has to be adjusted so that the background signal is as weak as possible compared to the measured signal. This ratio is influenced by several factors like the probe and its fluorescence properties, the staining or fixation protocols, the liquid handling or the number of cells seeded per well. Each of the variation of these parameters has to be evaluated with image analysis solution in order to define their influence on assay read-out. The assay has to be highly reproducible and controls should carefully be chosen and analyzed as they have strong influence on the meaning of the assay. They should reliably correspond to the phenotype of the biological activity to be tested so that obtained results are consistent with the biological question.

The choice of the probe has high consequences on the assay feasibility and quality. In fact, this choice mainly determines the protocol, the image analysis algorithm and also the cost of the resulting process. For instance, probes that imply long staining protocol or require computationally expensive image analysis solution will considerably lengthen the process and increase total cost of screen. Consequently, the whole HCS process has to be considered when an assay is set up and optimized.

Quality of assays are commonly estimated with z' factor[27]. This dimensionless statistical parameter represents the separation of the signal between the positive and negative populations and its definition is shown in Equation 1.

$$z' = 1 - \frac{3(SD_+ + SD_-)}{|\mu_+ - \mu_-|},\ 1 \le z' < -\infty$$

where, μ_+ and SD_+ the mean and the standard deviation of the positive control, μ_- and SD_- the mean and the standard deviation of the negative control

Equation 1. **z' factor definition.**

The z' factor quantitatively estimates the robustness of an assay by characterizing the screening window that could be used to identify hits. Positive z' values (with a maximum of 1) indicate that separation is possible between positive and negative populations unlike negative z' values, where these populations are merged. In HCS assay, every cell is analyzed and due almost infinite phenotype possibilities, outlier values commonly appear. Also, positive cell phenotype could append in negative control and vice-versa. These outliers usually have strong influence on the mean and the standard deviation and could dramatically lower z' factor.

1.5. High content-image analysis

High content screening produces images. If human eyes and brain can easily identify objects within an image, computerize this ability is a challenge. In order to get numerical data and be mathematically able to compare different cell phenotypes, images have to be analyzed. The automated image analysis process in HCS is called high content analysis (HCA). High content-image analysis aims to quantify the response of an assay by interpreting images and extracting data from those. The development of HCA has made possible high content screening, as this one is meaningful only if data can be obtained from the produced images. HCA is based on mathematical operations with picture elements (pixels); a particular HCA process is thus invariant and fully reproducible. Image analysis can be divided in three parts: image correction, image segmentation and feature extraction.[28]

Image analysis process typically starts with image corrections that aim to enhance image quality and create a more pronounced distinction between background signal and objects. Compensation of uneven illumination of the sample during image acquisition is a common step to improve image quality. In fact, imperfections of the optical system (e.g. slight component misalignment, dust) could create non-uniform illumination of the sample and thus differences in signal in the image only due to unequal excitation of the fluorophore. Flat field correction is used to compensate this effect and consists of correcting images with a reference image containing no sample. The reference image depends on the different optical components such objectives or laser lamps. An illustration of flat field correction is shown in Figure 4.

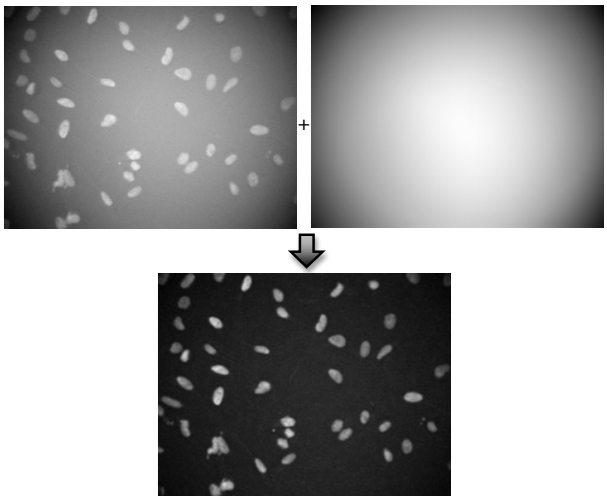

Figure 4. **Flat field correction.**

For each pixel of the acquired image, the flat field corrected corresponding pixel I_{corr} is defined as described in Equation 2.

$$I_{corr} = \frac{I_{ori}}{I_{ref}} \cdot m_{ref}$$

where, I_{ori} the intensity of the pixel in the original image, I_{ref} the corresponding pixel value in the reference image and m_{ref} the median of the reference image

Equation 2. **Calculation of the flat field correction.**

Constant value background subtraction can be used to minimize background signal. However, this method can alter the signal by flattening informative pixels and therefore has to be avoided as possible. Smoothing filters can be applied to reduce noise induced by acquisition system but they have to be carefully parameterized so they do not blur edges of objects or

remove small area informative objects. As a general rule, raw images must always be stored in case some processes altered the information contained in the images.
The main part of image analysis is image segmentation in which objects are segregated from the background signal. The simplest method to distinguish objects from background is to set an intensity threshold that highlights only pixels with high intensities, which should represent objects. Adjacent pixels above the defined threshold are then considered to be part of the same objects. In fact, intensity histogram of image obtained with fluorescent cell-based assay should ideally contain two separated peaks, the background signal and objects signal. This method works well only with several assumptions that are: image is not overcrowded with objects and most objects are spatially separated, image illumination is flat (or efficiently corrected) and objects signal is separated from background signal. Image processing filters can be used to enhance general contrast of the image or put in evidence some shapes that have to be segmented. Edge detector or sharpen filters could be useful to detect objects and increase intensity separation with adjacent elements, making thresholding easier. Segmented objects or shapes are often called region of interest (ROI). Once objects are segmented and their contours are spatially defined, their area can be calculated and thresholds can be set to remove small and large objects that could be noise or aggregates of the target shape. Watershed is a popular algorithm used to separate objects and the idea behind this algorithm is based on topography. Local maxima (objects) and minima (background) are considered respectively as hills and valleys and this imaginary landscape is filled with water. As level of water increases, valleys are flooded and the hills that stay out of water at a certain level are defined as objects.[29] This iterative algorithm has to be moderately used, as needed computational resource can rapidly increase like for other segmentation methods. For instance, segmentation based on edge tracing algorithm or using morphological templates fitted on the image are computationally expensive and might be not appropriate for HCA. A combination of simple thresholding and light version of these algorithms is often used to improve segmentation.
Unlike human eyes that are only sensitive to relative intensity values, computers can easily determine absolute intensity of regions within an image. This ability is used to extract different features of the segmented objects. Intensity (e.g. mean, median, standard deviation), shape (e.g. area, perimeter), surface (e.g. granularity, texture) and distribution (e.g. mean distance between objects) features can be calculated in the ROI obtained by segmentation. These values are used to characterize the phenotypes encountered in each image and have to be relevant to the biology behind. Most of the time, the more features are extracted, the more precise the classification is. However with hundreds of objects in image and hundreds to thousands images in a screen, the volume of data generated by these features can be huge and has to be monitored.
HCA is a difficult and crucial part of the HCS process and can be a bottleneck to this type of screening. To keep high throughput, image quality is often lowered and harden image analysis. A generic solution for all image analysis is not conceivable as every segmentation problem is different. Errors of segmentation have to be considered in data analysis and compensated by statistically significant number of observations. The HCA process has to be evaluated in time and computational resources as they have high repercussions on the quality and the cost of a screen.

2. Materials and methods

2.1. Cell culture

Henrietta Lacks (HeLa) cells were maintained in adherent flask culture during the whole length of the project. The cells were originally purchased at American Type Culture Collection (HeLa CCL-2) and grown at 37°C in humidified incubator containing 5% CO^2. The medium used was Dulbecco's Modified Eagle Medium + GlutaMAX™ (Invitrogen, Carlsbad, CA, ref. 32430) supplemented with 10% heat inactivated fetal bovine serum (origin: Australia, Invitrogen, Carlsbad, CA, ref. 10101-145).
Typical passage rate was twice a week with a dilution of 1:10 in 75 cm^2 flasks (Techno Plastic Products, Trasadingen, Switzerland, ref. 90076). Passaging was done by removing old medium, washing cells with phosphate buffer saline pH 7.4 (Invitrogen, Carlsbad, CA, ref. 10010) and detaching the cells with trypsin-EDTA (Invitrogen, Carlsbad, CA, ref. 25300) for around 10 min at 37°C. One milliliter of cell solution was then usually diluted in 9 ml of fresh medium heated at 37°C. Cell concentration was determined in the rest of the solution by counting in hemocytometer and cells were plated at a defined concentration to perform experiments. Different passage rates and dilutions were used to get enough cells for some experiments. When the number of passage was about 50, a new vial of lower passage number cells was thawed and re-cultured as described above.

2.2. Cell death inducers

Toxic molecules were used to induce cell death in HeLa cells. Three different protocols were tested to determine half lethal concentration (IC_{50}) for an initial population of 3'000 cells per well added as 90 µl in 96-well plates:

- Cell death inducer was added as 10 µl at the same time that the cells and incubated 24h.
- Cell death inducer was added as 10 µl 24h after the cells were plated and incubated 48h.
- Cell death inducer was added as 10 µl 48h after the cells were plated and incubated 24h.

Cell viability was then determined using alamarBlue® assay by adding 10 µl of alamarBlue® (AbD Serotec, Kidlington, UK, ref. BUF021A) and incubate 4h at 37°C. The alamarBlue® is composed of resazurin, a permeable non-fluorescent substrate that is reduced by living cells, producing resorufin a red fluorescent product. Quantification of resorufin fluorescence was done using Safire^2 (Tecan, Männedorf, Switzerland) with excitation/emission filter 560/590 nm and can be used to determine the viability of the cell population by comparing fluorescence emission with appropriate controls. The positive control (dead cells) was $CuSO_4$ 10^{-2} M and negative control (living cells) was chosen according to the solvent of death inducer (either H_2O or DMSO 0.3%). These different protocols were tested to get precise and time-dependent IC_{50} so that they are consistent with the assay to perform.
The following list shows cell death inducers tested and their reference:

- Ethylenediaminetetraacetic acid (EDTA) (Sigma-Aldrich, St. Louis, MO, ref. E5134)
- Gambogic acid (GBA) (Tocris Bioscience, Bristol, UK, ref. 3590)
- Sodium azide (NaN_3) (Sigma-Aldrich, St. Louis, MO, ref. S2002)
- Staurosporine (Roche, Basel, Switzerland, ref. 11055682001)
- Terpinen-4-ol (Sigma-Aldrich, St. Louis, MO, ref. 86477)
- Celastrol (Cayman Chemical, Ann Arbor, MI, ref. 70950)

2.3. Probes

The different fluorescent probes were handled and stored as advised by the providers. The list below shows the used probes where the were purchased:

- Hoechst 33342 (Invitrogen, Carlsbad, CA, ref. H1399)
- 4',6'-diamidino-2-phénylindole (DAPI) (Sigma-Aldrich, St. Louis, MO, ref. D9542)
- Calcein AM (Invitrogen, Carlsbad, CA, ref. C3100MP)
- Ethidium homodimer-1 (Invitrogen, Carlsbad, CA, ref. E1169)
- FLICA (Invitrogen, Carlsbad, CA, ref. I35106)
- Annexin V conjugate with Alexa Fluor® 488 (Invitrogen, Carlsbad, CA, ref. A13201)
- LC3B rabbit antibody (Invitrogen, Carlsbad, CA, ref. L10382)
- Anti-rabbit antibody labeled with Alexa Fluor® 647 (Invitrogen, Carlsbad, CA, ref. A21244)

These probes were tested on HeLa cells in 96-well plates and optimization was done according to the procedure described below.

2.4. Staining optimization

The aim of staining optimization is to get a maximal ratio between the signal one wants to observe and the background signal so that the signal for the positive and negative populations are separated enough for discrimination. Almost every step of the HCS process influences the read-out, from the number of plated cells to the segmentation parameters. The optimization was done by varying these different parameters that change the way a probe will be localized on its target and estimating how the positive and negative populations are separated. These parameters could be probe concentration, probe solvent, incubation time, incubation temperature or number of washes. For most of the probes, a starting protocol was defined by looking on provider documentation for the product or in the literature. From this protocol, parameters were slightly to broadly changed and staining quality was estimated for these conditions. HeLa cells in 96-well plates were used to perform these tests, typically at a concentration of 3'000 cells per well the day before the assay was done. The staining protocol are shown in Appendix 6.2.

Fluorescent probe staining often requires one or several wash steps in order to minimize background fluorescence of the probe diluted in the medium. When working on adherent cell culture in multi-well plate, these wash steps are usually performed with liquid handlers that remove a certain amount of medium in each well and refill the wells with liquid to dilute the primary medium. A problem that could arise from these steps is the detachment of cells that are aspirated by the liquid handlers generating loss of data or biased population. Especially when cells are dead, they naturally detach from well and thus are easier aspirated. Wash protocol validation was done by killing the cells with 10 mM $CuSO_4$ for 24h and staining cells with Hoechst. Initial concentration was estimated by acquire images of cells that have been homogenized by pipetting 3-4 times up and down and centrifuged for 2 min at 1000g. The wash step when then performed with different protocols on ELx405™ Microplate Washer (BioTek, Winooski, VT) and Biomek® 3000 Laboratory Automation Workstation (Beckman Coulter, Brea, CA). Cells were homogenized and centrifuged again and imaged to estimate percentage of remaining cells. The wash efficiency (percentage of dilution of the initial medium) was measured by spectrofluorometry with 200X fluorescein, which fluorescence was acquired with Infinite® F500 (Tecan, Männedorf, Switzerland) before and after wash.

2.5. Automated microscopy

The automated microscope used was a BD Pathway™ 855. This fluorescence microscope offers a wide range of visualization spectra (340 nm to 750 nm) thanks to dual-mercury metal halide lamps. The light path can be set up as wide field or it is possible to take spinning disk images. Temperature and carbon dioxide controls inside imaging chamber allow time-lapse microscopy with living sample. A basic liquid handling module is present and can be used to add a reagent for instance when imaging should starts directly after the addition of a reagent for short term reactions.

An image analysis software called Attovision™ is also provided. This software allows the controls the different part of the microscope like motorized objective, light paths or liquid handling module and let build macros for automation of imaging. These macros were used for imaging and typically started with autofocus command composed either of two image-based autofocus (coarse and fine) or laser-based autofocus and fine image-based autofocus. In laser-based autofocus, the bottom position of the plate is found thanks to the change of refractive index between the transition air-plastic and plastic-medium. This type of autofocus is faster than image-based autofocus, which consists of acquiring images at different Z positions and use image processing algorithm (Vollath F4) to define which image is in focus thanks to estimation of image sharpness and contrast. The focus position was found on nuclear stain and the other lightpaths were acquired at this position. A montage of 2x2 or 3x3 images with 20X objective was usually set up to get a larger sample of each well. All images were acquired with a 20X objective, Universal Apochromatic, NA: 0.75, xyFOV 420 x 320 µm, Olympus (Shinjuku, Japan, ref. UAPO20X/340) if no other mention.

The software also provides segmentation capabilities and data analysis features. To find cell position and cell number, nuclear stain image was used. After flat field correction, image processing algorithms RB 25X25 (rolling ball) and shading (algorithms not disclosed) were applied to respectively reduce background and sharpen image by equalizing intensity of bright objects. A threshold was then set to discriminate between background and cell nuclei. This threshold was relative to mean intensity of each image and was automatically adapted if an image was brighter or darker. Watershed was used to split nuclei that were too close to be separated by intensity thresholding. Finally, objects with smaller or bigger area than defined thresholds were discarded, as they either were debris or aggregates of nuclei that were not split by watershed. Whole cell was defined by dilation of nine pixels from nucleus border. This segmentation resulted in two ROI: cell nucleus and whole cell. These ROI were used for measurements in the different images acquired with the lightpath corresponding to the probes. A two-steps segmentation was necessary to get whole cell ROI and nucleus ROI (see Figure 5) because of limitation of the software. Exact parameters of segmentation are shown in Appendix 6.3.

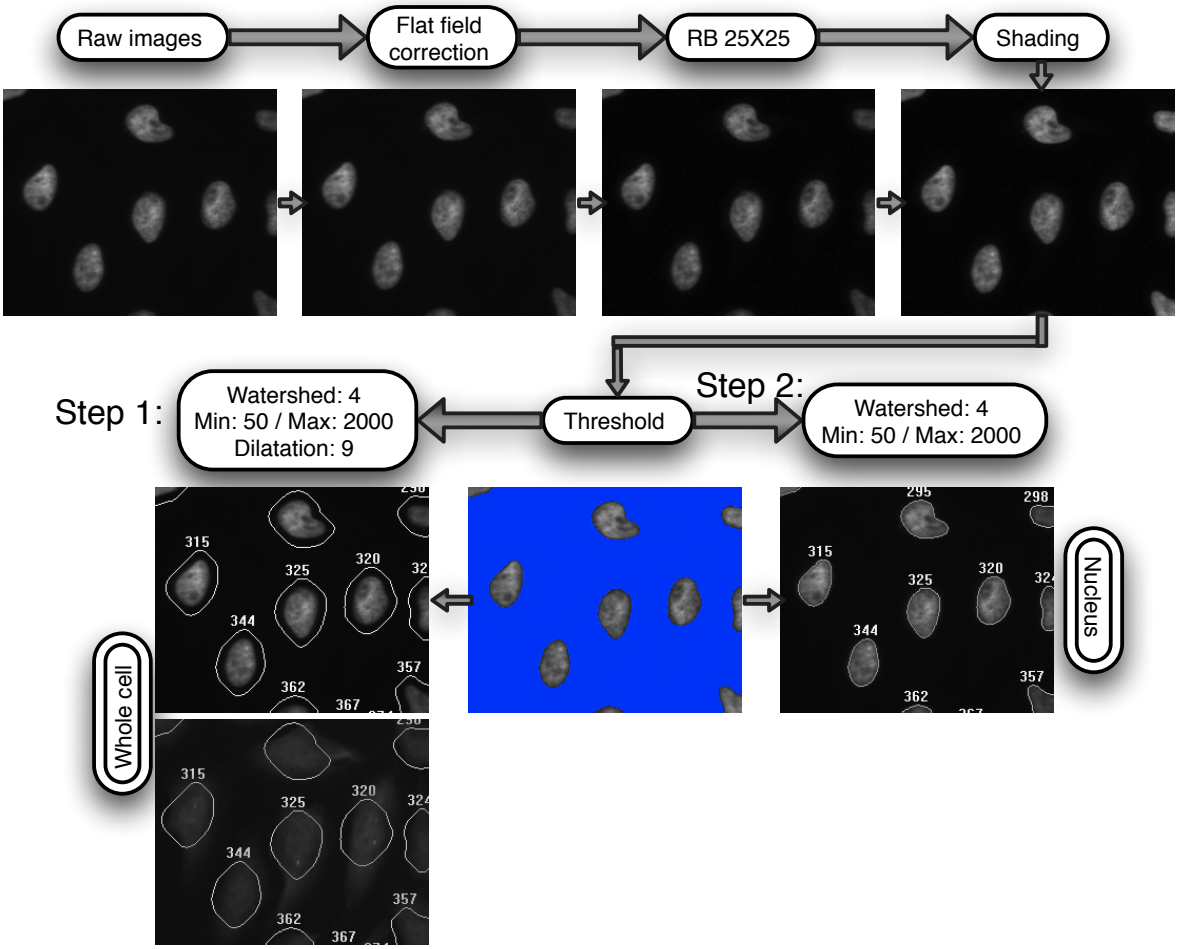

Figure 5. **Segmentation process.**

First step of segmentation aims to define whole cell mask. After flat field correction, RB 25X25 is used to remove background. Shading allows brightening objects with low intensity. A threshold is then set to discriminate between background (shown in blue) and nuclei. Dilatation of 9 pixels is used to define whole cell. The second step of segmentation use the same parameters without the final dilatation to define cell nucleus.

2.6. Data analysis

After image segmentation, different features were extracted depending on the assay performed. Parameters like mean pixels intensity within a ROI, total area or intensity variations in a ROI were typically measured to characterize each object found in segmentation. Attovision™ wrote output data in a text file containing each object in row and its parameters in the corresponding column for each well analyzed. The different wells were horizontally separated by several rows containing information on the used lightpath and other acquisition parameters. As this data configuration was not favorable to data handling and analysis, a Visual Basic® for Applications macro was coded in Microsoft® Office Excel to re-organize data in a way that makes easier their manipulation. Data were organized by well in adjacent columns and objects with their parameters in rows. The macro also removed some ROI automatically generated by Attovision™ to enhance data visibility. To get a fast overview of plate response map, mean value of the different parameters extracted were also automatically computed for each well and written in separate sheet. A second macro was

coded to gather all images of an experiment together in a single folder as Attovision™ placed these images in a not user-friendly arborescence of folders. Information and user guideline of these macros can be found in Appendix 6.4.
The aim of data analysis was to find the threshold that defined positive and negative populations for cells stained with a probe. For this purpose mean signal and variation of positive and negative controls were computed. Relevant features extracted from segmentation should show distribution shift between positive and negative controls as shown in Figure 6.

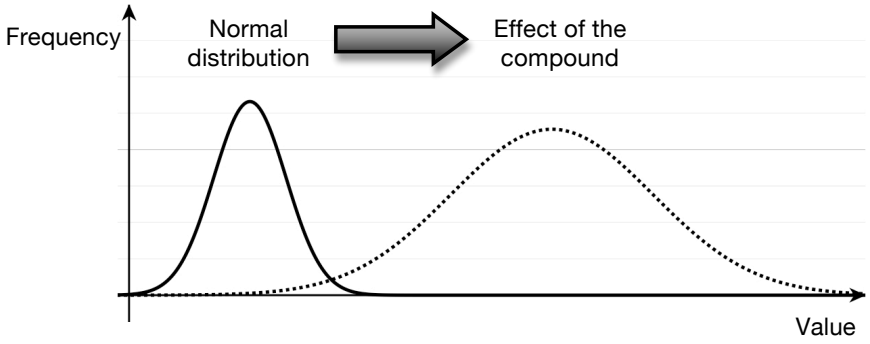

Figure 6. **Typical distribution of value in an assay.**

Normal response of a biological system to an assay compared to a positive distribution. Positive compounds should induce a change in mean signal of the parameter measured.

For intensity measurements, negative control represented usually mean background signal of the image, as most of the cells should not be stained with the used dye. However, some positive cells might be found in negative control and in order to find a threshold that really corresponds to negative signal, outlier values were removed from mean and standard deviation computation. For a dataset $[x_1, x_2, \ldots, x_n]$ sorted in ascending order, outliers were defined as shown in Equation 3.

$$x_i > Q_3 + \frac{3}{2}(Q_3 - Q_1) \quad \text{or}$$

$$x_i < Q_1 - \frac{3}{2}(Q_3 - Q_1), \quad \text{for } 1 \le i \le n,\ i \in \mathbb{N},$$

where,

$$Q_p = x_k + d \cdot (x_{k+1} - x_k), \quad k = \left\lfloor \frac{p}{4}(n-1) + 1 \right\rfloor \text{ and}$$

$$d = \frac{p}{4}(n-1) + 1 - k, \quad \text{for } 1 \le p \le 3,\ p \in \mathbb{N},$$

Equation 3. **Outliers definition.**

In other words, values that were 1.5 times the inter-quartile distance over the superior quartile and the same distance below the inferior quartile were removed for mean and standard deviation computation. Three standard deviations over and below mean exclusion could also have been used but this method took more in account the distribution of the data that was often present in staining experiment. For instance in negative control, this distribution could typically be represented by two Gaussians: most cells were distributed around the mean of negative signal and few cells that were positives created a small Gaussian-like distribution with a mean close to positive response. The described procedure corrected this effect most of the time to get a mean value and standard deviation corresponding the positive or negative populations. Thresholds were then set usually at three standard deviations from the corrected

mean to define the criterion of membership to a population. These thresholds were checked by going back to some images and estimating by eyes classification if the right population was segregated with the defined criterions.
The relevance of a features extracted from image segmentation was estimated by computing z' factor using the positive and negative controls. In fact the higher the separation between the positive and negative distributions was, the more certain the classification of cells in each populations was.

3. Results

3.1. Staining results

3.1.1. DAPI and Hoechst

The nuclear probes Hoechst 33342 and DAPI were tested and optimized for HeLa cells in 96-well plate. Hoechst staining was tested within a concentration range from 0.25 μg/ml to 40 μg/ml, incubation time from 5 min to 45 min, incubation temperature 37°C/room temperature (RT), with 0X/1X wash with PBS and on living/dead cells.
The probes showed homogeneous nuclear signal after 15 min at 37°C and about 30 min at RT. With lower incubation times, the nuclei of cells were stained only on their border showing that the diffusion and fixation process of the probe was not advanced enough. The signal within cell nucleus was about 5-8 times higher than the background signal with Hoechst concentration above 1 μg/ml, giving wide possibility of thresholding to distinguish nuclei from background. Each of the cited conditions above with this concentration range gave the possibility to efficiently segment cell nuclei from background signal, the main purpose of nuclear staining. When the concentration was below 1 μg/ml, segmentation was less efficient because cell nuclei intensity was about 1.5 to 3 times higher than background. For these concentrations, exposition time was increase from around 0.008 s to 0.03 s so that the signal was detectable by the CCD camera. The wash step showed no significant improvement of signal-to-background ratio. Cytoplasm intensity was comparable to background signal proving high specificity of Hoechst to DNA.
To minimize acquisition time and quantity of used probe, the final optimal concentration further used for this project was set at 1 μg/ml. The optimal parameters are summarized in Table 4.

Hoechst staining		
Parameter	**Value**	
Final concentration	1 μg / ml in H_2O	
Incubation time	15 min	30 min
Incubation temperature	37°C	RT
# of wash required	0X	
Approximative exposure time	0.008 s	

Table 4. **Hoechst staining parameters.**

Similar optimization was done for DAPI staining. As shown in Figure 7, it appeared that background signal was more intense than in Hoechst staining with a ratio of about 1.2 between cell nuclei and background even with flat field correction. The wash step with 100 μl PBS per well significantly improved this ratio by increasing it between 4-6, a similar result to Hoechst staining. This phenomenon might be due to lower lipophilicity of DAPI compared to Hoechst as explained in Chapter 1.3.1.

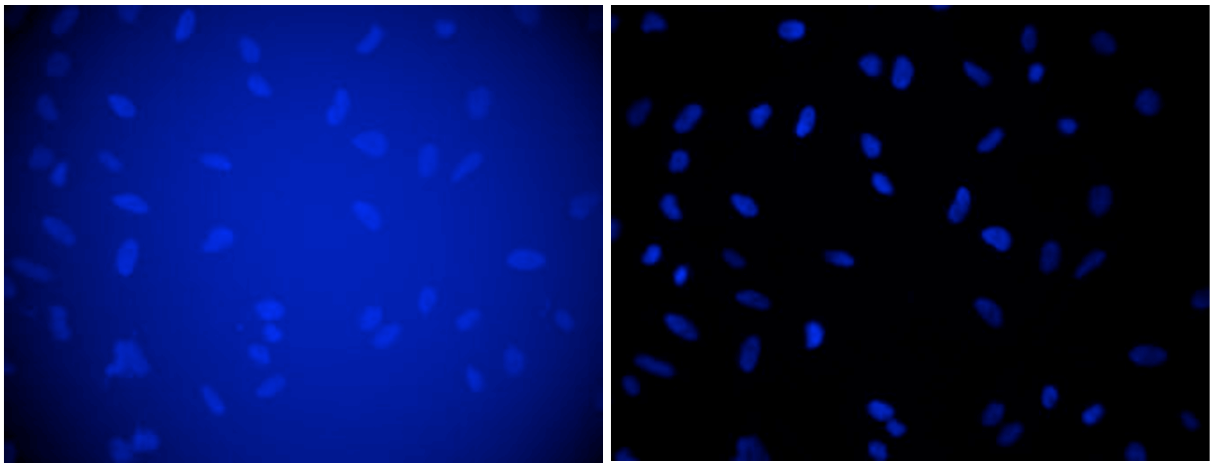

Figure 7. **Need for a wash step in DAPI staining.**

The left side of the figure shows HeLa cells stained with 10 µg/ml DAPI after 20 min incubation at 37°C. On the right side, the same cells after one wash with 100 µl of PBS.

The incubation time and temperature were similar to Hoechst and optimal concentration was 10 µg/ml. These parameters are shown in Table 5.

DAPI staining		
Parameter	**Value**	
Final concentration	10 µg / ml in H_2O	
Incubation time	15 min	30 min
Incubation temperature	37°C	RT
# of wash required	1X	
Approximative exposure time	0.01 s	

Table 5. **DAPI staining parameters.**

Except from cell number and position, another feature that could be extracted from nuclear stain was nucleus shape. In fact as shown in Figure 8, the nucleus of cells has a different morphology when the cell is viable, apoptotic or necrotic. Cell nucleus also adopts distinct morphology during the mitotic process and depends on cell cycle. Viable cells showed uniform nuclear stain with almost regular oval shape. For necrotic cell nucleus, the staining intensity was higher than in viable cells and nuclear area was reduced. Characteristic nuclear fragmentation was observed in apoptotic cells, as their nucleus contained small bright dots. This information that can be used to get insights of cell state is further depicted in Chapter 3.2.2.

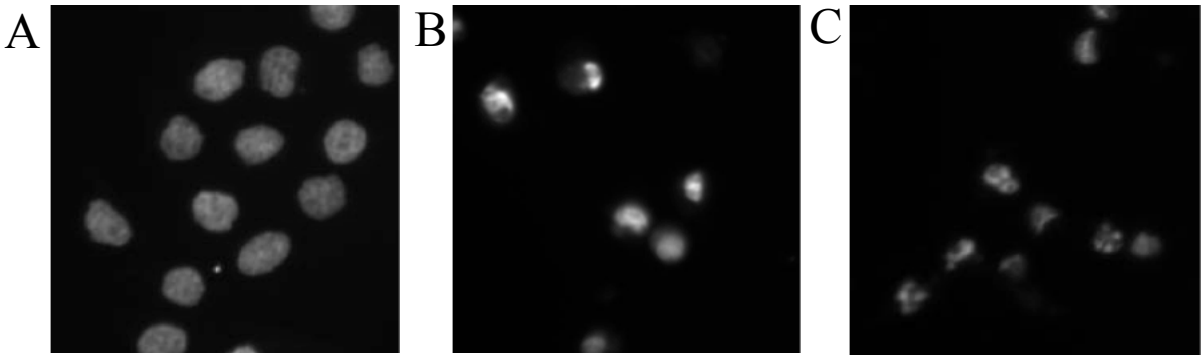

Figure 8. **Hoechst staining showing nuclear morphology of viable, necrotic and apoptotic cells.**

HeLa cells stained with Hoechst 1 μg/ml. **A.** Viable cells. **B.** Cells treated with 10 mM $CuSO_4$ for 24h at 37°C (necrotic cells). **C.** Cells treated with 10 μM staurosporine for 4h at 37°C (apoptotic cells).

3.1.2. Calcein and EthD-1

Calcein staining was optimized for HeLa cells in 96-well plate. The parameters tested were: concentration range [0.0625 – 4 µg/ml], solvent PBS/water, incubation temperature 37°C/RT and incubation time from 20 to 60 min. Hoechst 33342 staining was first chosen as nuclear probe to identify cell number and position as it seemed more efficient than DAPI. Nevertheless, it appeared that when Hoechst was used with calcein, the repartition of calcein within cell cytoplasm was not homogeneous and aggregates were presents in medium. As shown in Figure 9, DAPI had not this effect on calcein and was thus chosen as nuclear stain for calcein assays.

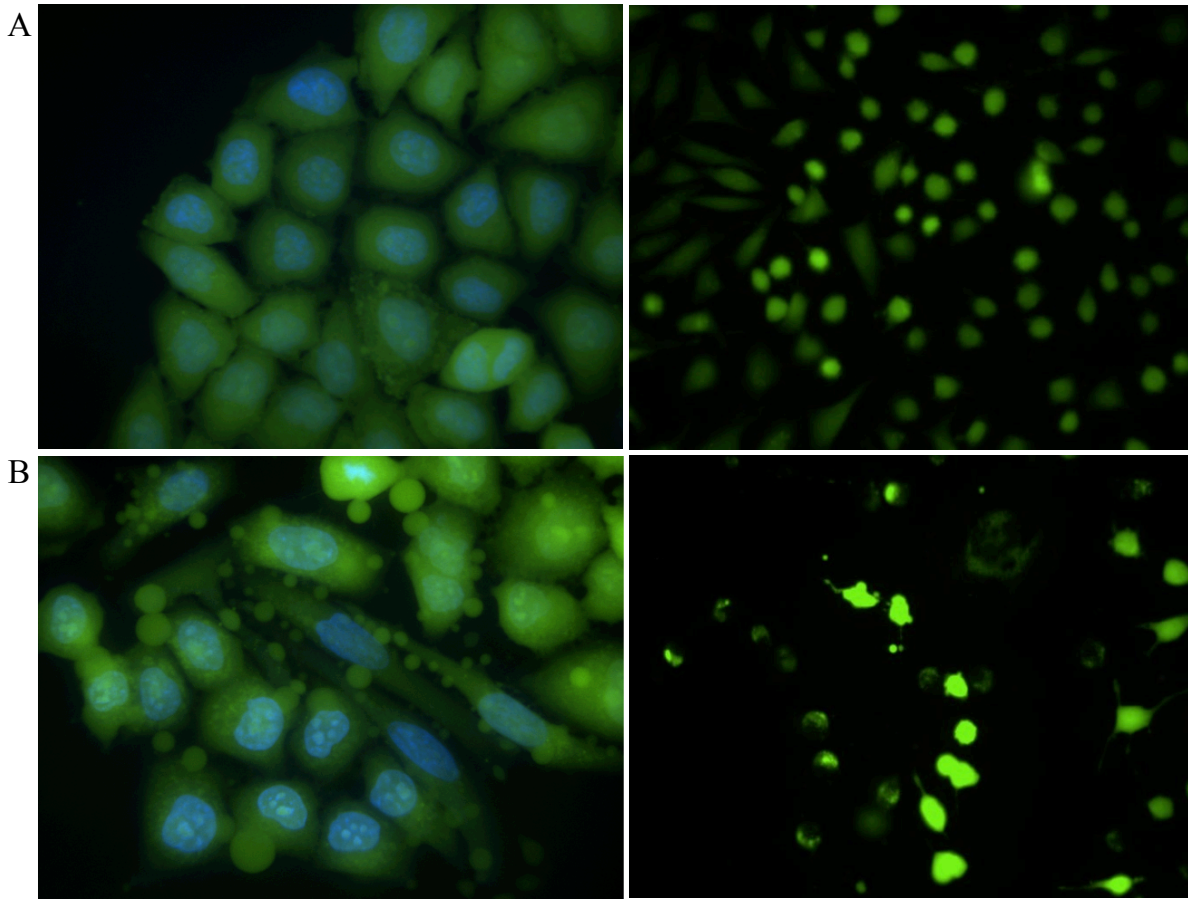

Figure 9. **Calcein-AM staining is degraded by Hoechst but not by DAPI.**
HeLa cells stained with **A.** 10 µg/ml DAPI (cyan) and 0.5 µg/ml calcein-AM (green). **B.** 1 µg/ml Hoechst (cyan) and 0.5 µg/ml calcein-AM (green). The upper and lower corresponding images are extracted from the same plate and thus have the same experimental conditions. The two left images are acquired with a 40X objective.

The lower concentration of calcein that allowed decent segmentation was 0.5 µg/ml and no significant differences was observed when the solvent was PBS or H_2O. Incubation time was found to be minimum 30 min at 37°C and 45 min at RT so that esterase activity was detectable. Residual fluorescent calcein was present in dead cells and was partly removed by one wash with 100 µl of PBS. The wash step also diminished the background signal due to the esterase activity of FBS present in medium. The parameters are summarized in Table 6.

Calcein staining		
Parameter	**Value**	
Final concentration	0.5 µg / ml in H_2O	
Incubation time	30 min	45 min
Incubation temperature	37°C	RT
# of wash required	1X	
Approximative exposure time	0.01 s	
Notes	Do not use with Hoechst 33342	

Table 6. **Calcein staining parameters.**

The nucleic acid probe EthD-1 was tested on HeLa cells in 96-well plate with concentrations between 0.125 µM and 12 µM. The best concentration found was 1 µM with incubation time of 30 min at 37°C and 50 min at RT. Cell death was first induced by treatment with 70% ethanol at – 20°C for 15 min to get rapid death and so that cells stayed attached. As shown in Figure 10, the phenotype of cells killed by this way does not correspond to most of dead cell shape. In fact, cytoplasm of cells looked intact as they were fixed whereas "natural" dead cells adopted round shape. Thus, the control was changed to 10 mM $CuSO_4$ incubated 24h.

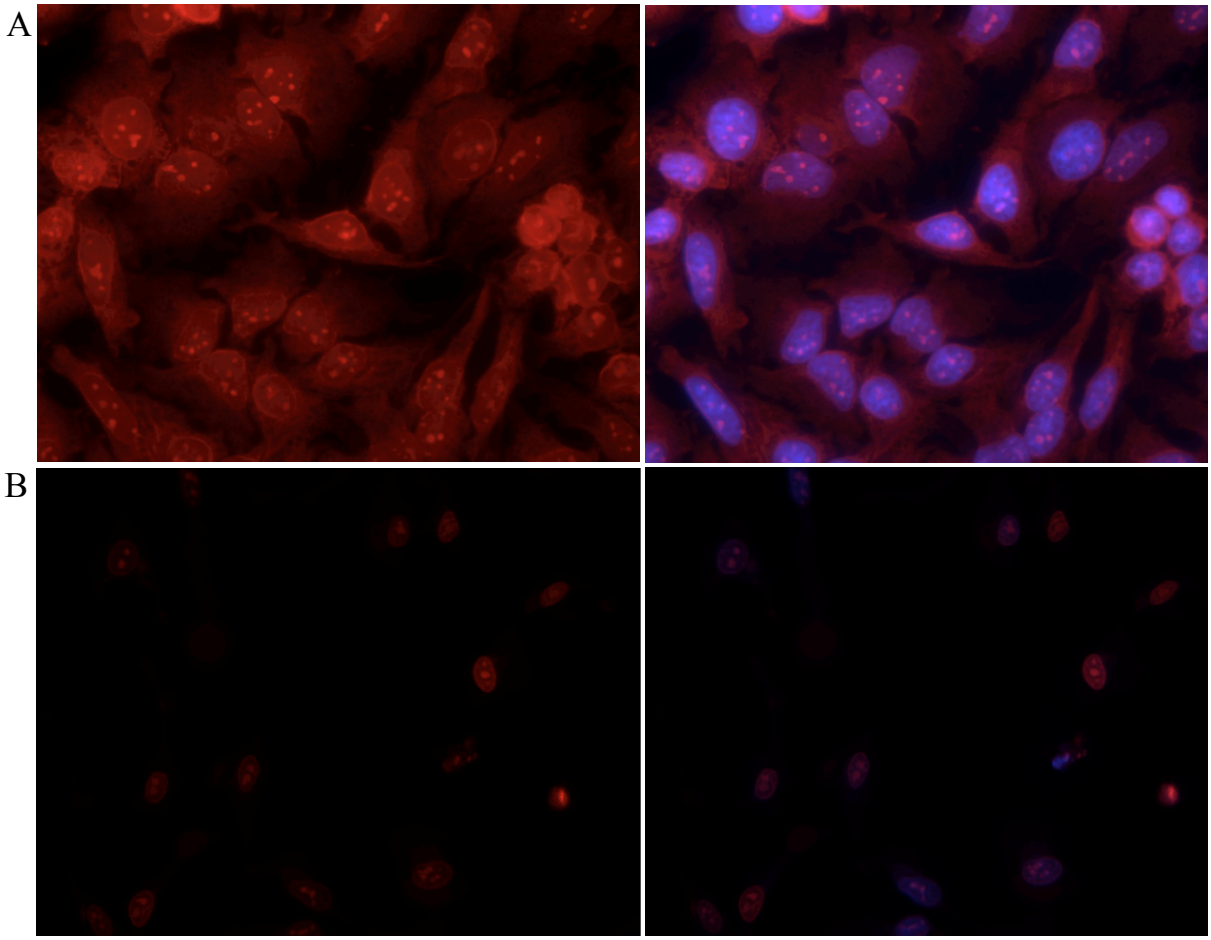

Figure 10. **EthD-1/Hoechst dual staining of cells treated with – 20°C EthOH and staurosporine.**

HeLa cells stained with 1 µM EthD-1 (red) and 1 µg/ml Hoechst (blue). **A.** Left: red channel of cells treat with 70% EthOH at – 20°C for 15 min. Right: same image merged with blue channel. **B.** Left: Red channel of cells treated with 10 µM staurosporine for 10h. Right: same image merged with blue channel.

Another phenomenon that could appear is competition between nuclear probe and EthD-1 as both of them bind to DNA. Comparison of the addition of EthD-1 10 min before Hoechst with further incubation of 20 min at 37°C and both dyes added together incubated 30 min at 37°C was done to control this effect. EthD-1 staining showed no significant difference between the two protocols performed on the same plate. Staining parameters with EthD-1 are shown in Table 7.

EthD-1 staining		
Parameter	**Value**	
Final concentration	1 µM in H_2O	
Incubation time	30 min	50 min
Incubation temperature	37°C	RT
# of wash required	0X	
Approximative exposure time	0.03 s	

Table 7. **Ethidium homodimer-1 staining parameters.**

The combination of the three probes (calcein-AM, EthD-1 and DAPI) was tested at the defined concentrations with incubation time of 30 min at 37°C. This assay use intracellular esterase activity and membrane permeability to discriminate between living and dead cells and best images of this test are shown in Figure 11.

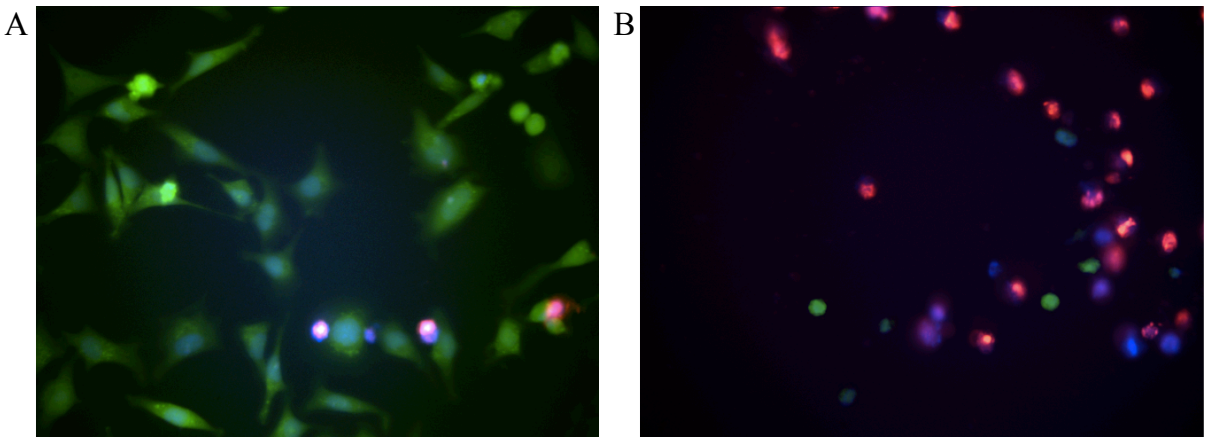

Figure 11. **Live/dead assay with calcein-AM, EthD-1 and DAPI.**

The figure shows HeLa cells stained with 0.5 µg/ml calcein (green), 1 µM EthD-1 (red) and 10 µg/ml DAPI (blue). **A.** Viable cells. **B.** Cells treated with 10^{-2} M $CuSO_4$ for 24h at 37°C (dead cells).

3.1.3. FLICA

The apoptotic indicator based on caspases activation FLICA was tested on HeLa cells in 96-well plate. The probe was combined with Hoechst to detect cell number/position and propidium iodide that stains late apoptotic/necrotic cells due to their damaged membrane. Kinases inhibitor staurosporine was used to induce apoptosis at a concentration of 10^{-4} M, 10^{-5} M, 10^{-6} M and 10^{-7} M. After 2h and 4h incubation with staurosporine, most of the cells were negative for FLICA staining and the signal for positive cells was low (see Figure 12A). Even with up to three wash steps, the background signal was high and to ratio with positive cells was about 1.2, which was not sufficient for efficient discrimination between apoptotic and living cells. Another test was performed with 6h incubation with staurosporine at the cited concentrations and the best images were most of the cells were positive for FLICA are shown in Figure 12B. The ratio between positive cells and background was increased to about 1.8 and the separation between positive and negative cells stayed difficult.

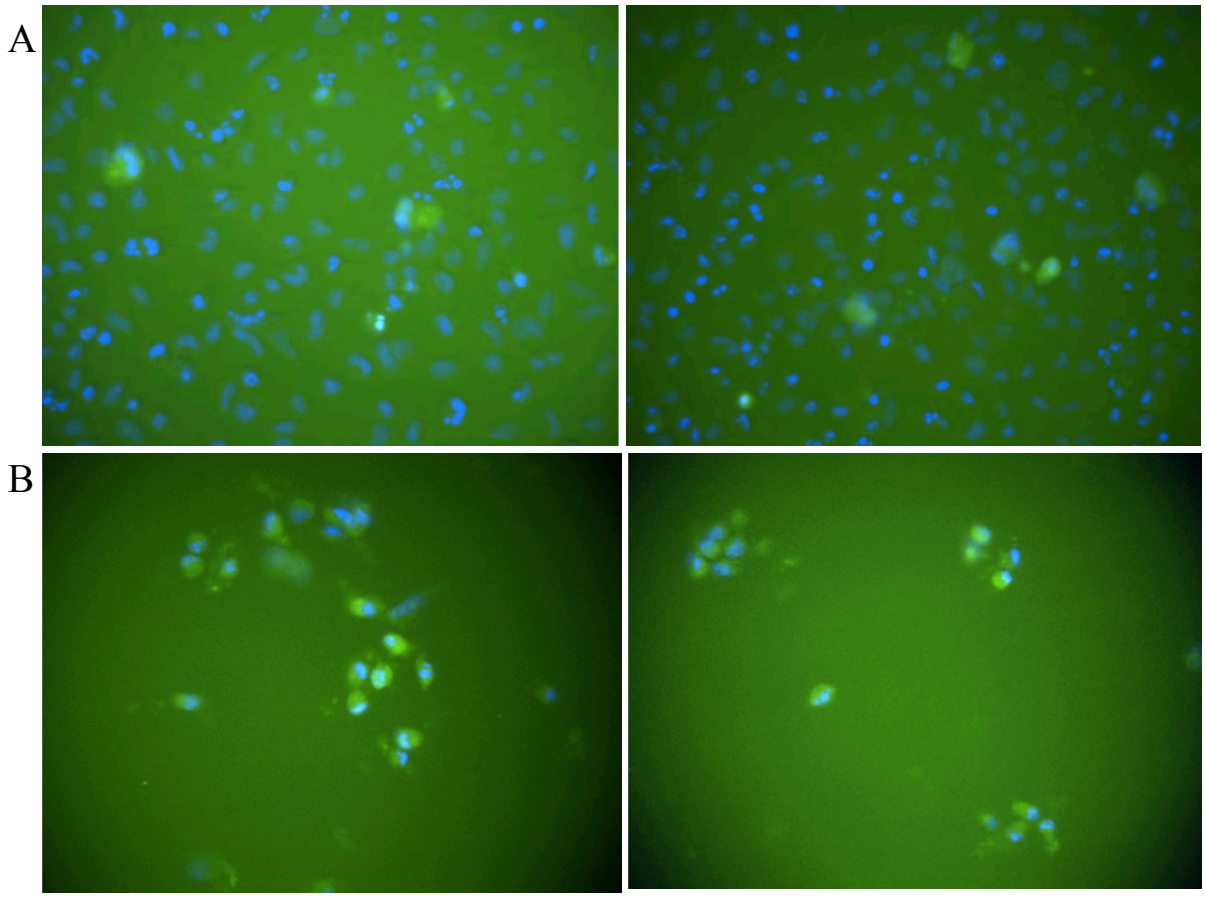

Figure 12. **FLICA staining.**

HeLa cells stained with FLICA. **A.** After 2h incubation with 10^{-5} M staurosporine. **B.** After 6h incubation with left: 10^{-4} M staurosporine and right: 10^{-5} M staurosporine.

3.1.4. Annexin V conjugate

Annexin V conjugate, a probe that binds to phosphatidylserine, was tested to detect apoptosis on HeLa cells in 96-well plate. Positive control was done by treatment with staurosporine, a kinase inhibitor known to induce apoptosis, at different concentration (10^{-4} M, 10^{-5} M and 10^{-6} M). The probe was combined with Hoechst and EthD-1 to detect cell with compromised plasma membrane (see Chapter 1.3.5). Tests were performed after 3h, 4h, 8h and 24h incubation with staurosporine and a time-lapse analysis was done by acquiring images every 8 min for 10 hours. The first experiment was done with 3h and 24h incubation of 10^{-4} M, 10^{-5} M and 10^{-6} M staurosporine. At 10^{-6} M, no apoptotic cells were detected after 3h and few dead cells (annexin V and EthD-1 positives) were present after 24h. This concentration was not high enough to induce apoptosis. At 10^{-5} M, nuclear fragmentation was observable in most of the cells and some were positives for annexin V staining after 3h. With the same concentration and 24h incubation, half of the cells were EthD-1 positive and a third of the population was positive for annexin V. When the concentration of staurosporine was increased to 10^{-4} M, half of the cells showed phosphatidylserine translocation after 3h and nuclear fragmentation was present in all cells. After 24h incubation at this concentration, most of the cells were dead with few of them still in apoptotic process. Thus, the concentration of 10^{-5} M was defined as reference for its similar time to induce apoptosis compared to what was found in literature. With higher concentrations, compounds that would trigger apoptosis in a longer period would be missed. An other test was performed with this concentration and an incubation time of 4h and 8h. With 4h incubation, a small half of the population was engaged in the apoptotic process. After 8h, almost all of the cells were positive for annexin V staining and negative for EthD-1 showing that the time of incubation was in the right order of magnitude.

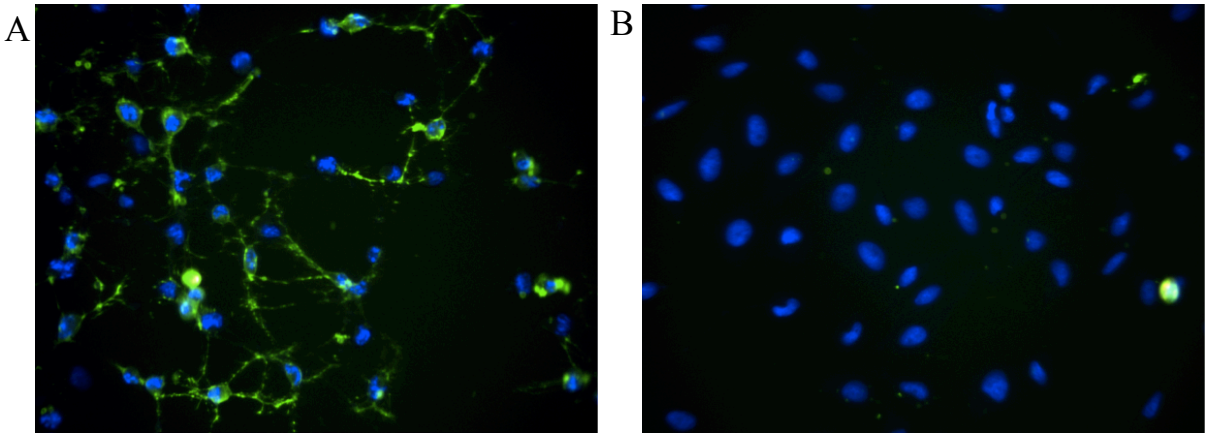

Figure 13. **Annexin V conjugate staining.**

HeLa cells stained with 50X annexin V conjugate (green), 1 µg/ml Hoechst (blue) and 1 µM EthD-1 (red) **A.** Cells treated with 10 µM staurosporine. **B.** Negative control.

Time-lapse analysis was performed to get insight of the timeframe in which phosphatidylserine translocation appends and cell membrane is still intact (Figure 14). Two conditions were tested: control and cells treated with 10^{-5} M staurosporine. After 3h30, the majority of cells treated with staurosporine were stained with annexin V conjugate and not with EthD-1. Cell membrane became permeable for most cells in these wells after around 6h. This timeframe was shorter than what was observed by end-point experiments. However, this time could be influenced by several apoptotic-inducing factors that are: presence of Hoechst 33342 and fluorescence imaging. Apoptosis induction by these factors was confirmed in

control wells that showed phosphatidylserine translocation in most cells after 5h and about half of the cells were positive for EthD-1 after 10h. Imaging capability to induce apoptosis was further confirmed as first apoptotic cells appeared at the center of the image, where auto-focus images were taken. Thus, these cells that received more irradiation by laser engaged apoptosis pathway before surrounding cells. This proves that the apoptosis induction and mechanism of phosphatidylserine translocation are time-dependent and their execution depends on the nature and the amount of inductors.

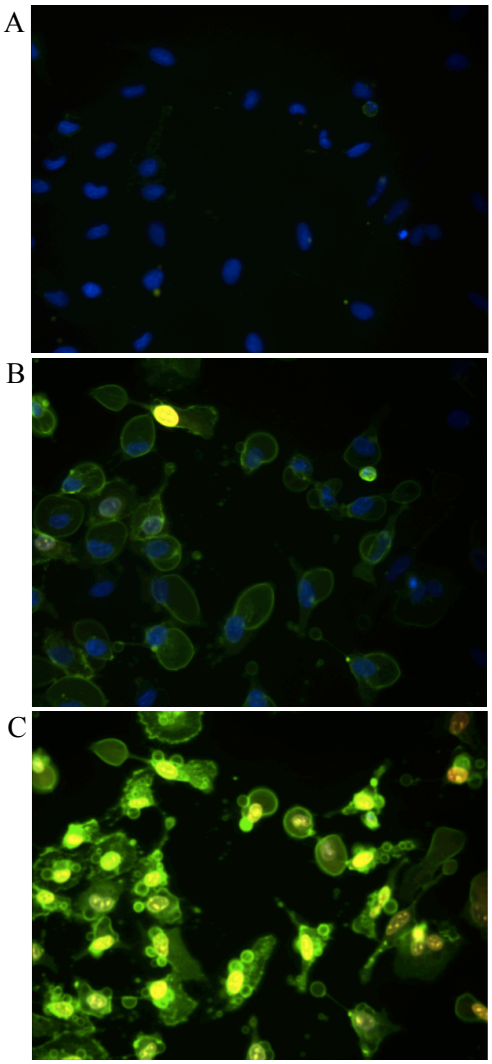

Figure 14. **Time lapse analysis of annexin V conjugate staining.**

Cells were stained with 1 μg/ml Hoechst (blue) for 15 min at 37°C. After 1X wash with 100 μl PBS, a solution of annexin-binging buffer (10 mM HEPES, 140 mM NaCl, 2.5 mM $CaCl_2$) containing 50X annexin V conjugate (green), 1 μM EthD-1 (red) and 10 μM staurosporine was added. Images of Hoechst (blue), annexin V conjugate (green) and EthD-1 (red) channels were taken every 8 min for 10h in chamber kept at 37°C and 5% CO_2. **A.** Time t=0. **B.** t=4h. **C.** t=10h.

3.1.5. LC3B antibody

LC3B immunostaining was tested to detect autophagosomes formation in HeLa cells in 96-well plate. Different concentrations of primary antibody (0.5 µg/ml, 1 µg/ml), secondary antibody (200X, 500X, 1000X, 2000X) and blocking buffer composition (Bovine serum albumin 1%, 2%) were used to estimate capability to detect autophagy. Precise protocol can be found in Appendix 6.2. Chloroquine, an anti-malarial and anti-inflammatory drug known to induce autophagy, was set as positive control and used at 30 µM, 50 µM, 100 µM incubated around 16h (overnight). At 30 µM, significantly less autophagosomes were present in the cytoplasm of autophagic cells compared to a concentration of chloroquine of 50 µM and 100 µM. Small differences were observed between 50 and 100 µM but a concentration of 100 µM was chosen as positive control in order to induce the maximum number of autophagosomes. When 0.5 µg/ml of primary antibody was used, the staining showed less specificity for autophagosomes with relatively high cytoplasm signal. A mean of 15% higher intensity ratio between autophagosomes and cytoplasm was obtained with a concentration of 1 µg/ml of primary antibody while other conditions were kept the same. For secondary antibody, this ratio was increased by around 12% by using a 200X dilution compared to 2000X. Augmentation of bovine serum albumin (BSA) in blocking buffer that avoid non-specific interaction of antibodies, did not increase this ratio as autophagosome intensity was also reduced with 2% BSA. The condition in which autophagosomes were the most clearly observable and easily segmented (see Figure 15), was thus 100 µM chloroquine, 1 µg/ml of primary antibody and 200X secondary antibody.

As chloroquine appeared to induce autophagosomes formation with overnight incubation, other incubation times were not tested. Incubation of primary and secondary antibodies (1h at RT, see Appendix 6.2) could also have been increased to enhance the signal but these times were kept as low as possible to meet screening requirements and to avoid making longer a already time-consuming protocol. Further optimization might be obtained by varying these different incubation times. Other parameters like concentration and incubation time of membrane permeabilizant (Triton-X100), fixation protocol or number of wash could also be investigated.

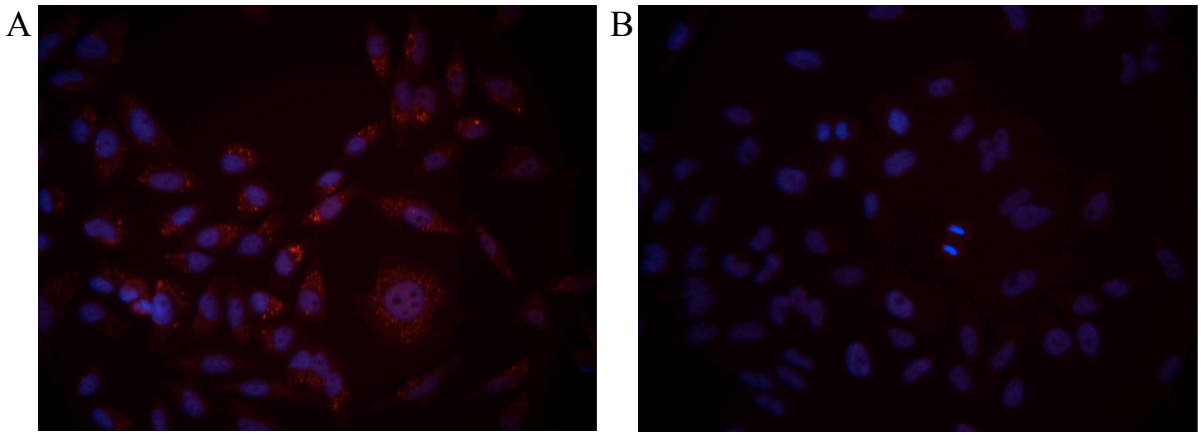

Figure 15. **LC3B immunostaining.**

HeLa cells stained with LC3B immunostaining (1 µg/ml primary antibody, 200X secondary antibody and blocking buffer 1% BSA). **A.** Treated with 100 µM chloroquine for 16h. **B.** Control.

3.2. Data analysis results

3.2.1. Wash protocol validation

Different wash protocols were tested on cells treated with 10 mM $CuSO_4$ for 24h. The percent of remaining cells after wash and the wash efficiency represented by the dilution of fluorescein are showed in Figure 16.

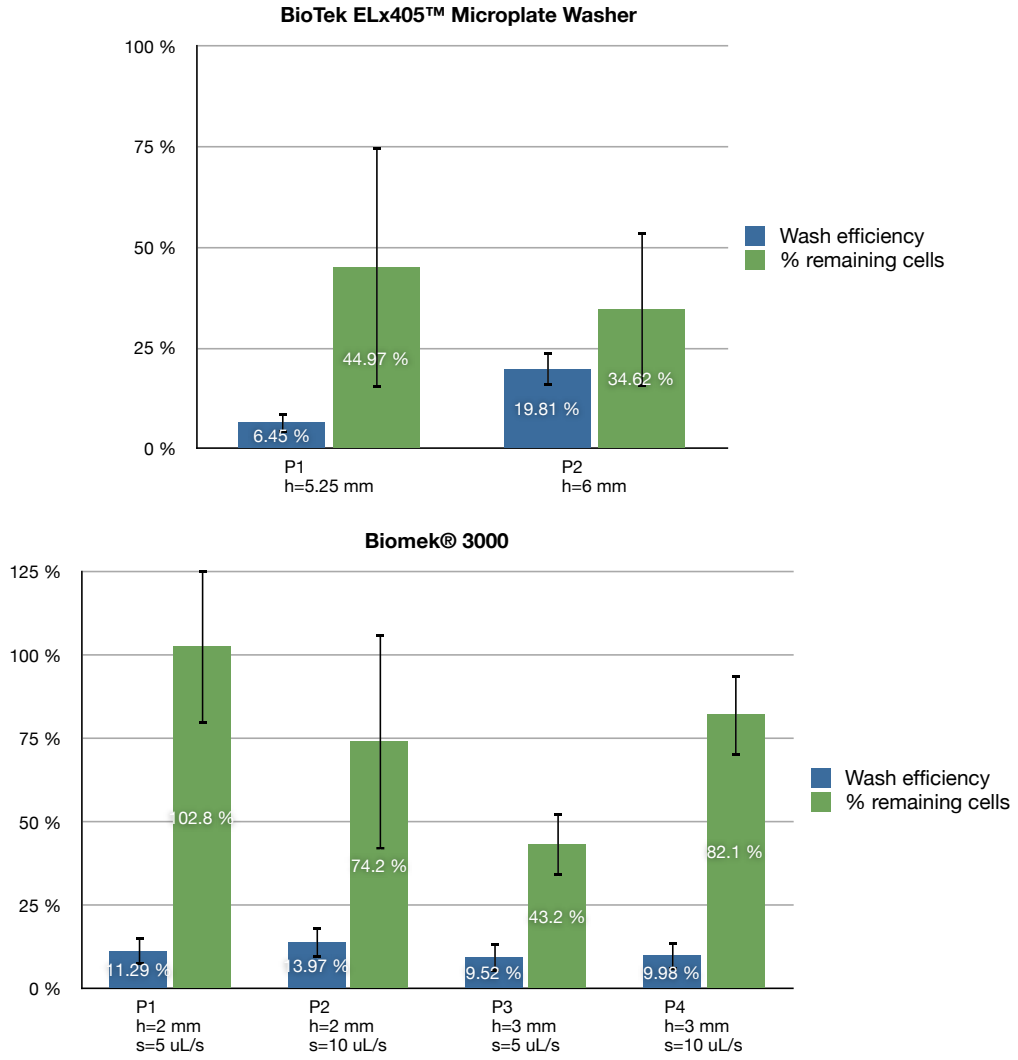

Figure 16. **Wash protocol validation results.**

The upper part shows wash efficiency and percentage of remaining cells for wash with two different protocols with BioTek ELx405™ Microplate Washer at aspiration height of 5.25 and 6 mm and lowest traveling speed within well. The lower part, the same results with BioMek® 3000 at aspiration height of 2 and 3 mm and aspiration speed 5 and 10 µl/s.

ELx405™ Microplate Washer removed more than 50% of the dead cells with all the tested protocols and was thus not suitable for working with cell viability assays. Other tests were performed with BioMek® 3000 and decent results were obtained with aspiration height of 2 mm and aspiration speed of 5 µl/s; with this protocol, almost all dead cells remained in well (mean: 102.8%) and wash efficiency was high with a mean of 11.3% remaining of the initial solution. However, high variations regarding cell number were observed in all protocols showing that the method was not optimal for reproducibility.

3.2.2. Nucleus characterization

HeLa cell nuclei were analyzed over different experiments. Some features that appeared to be relevant to cell viability were extracted and are shown in Figure 17.

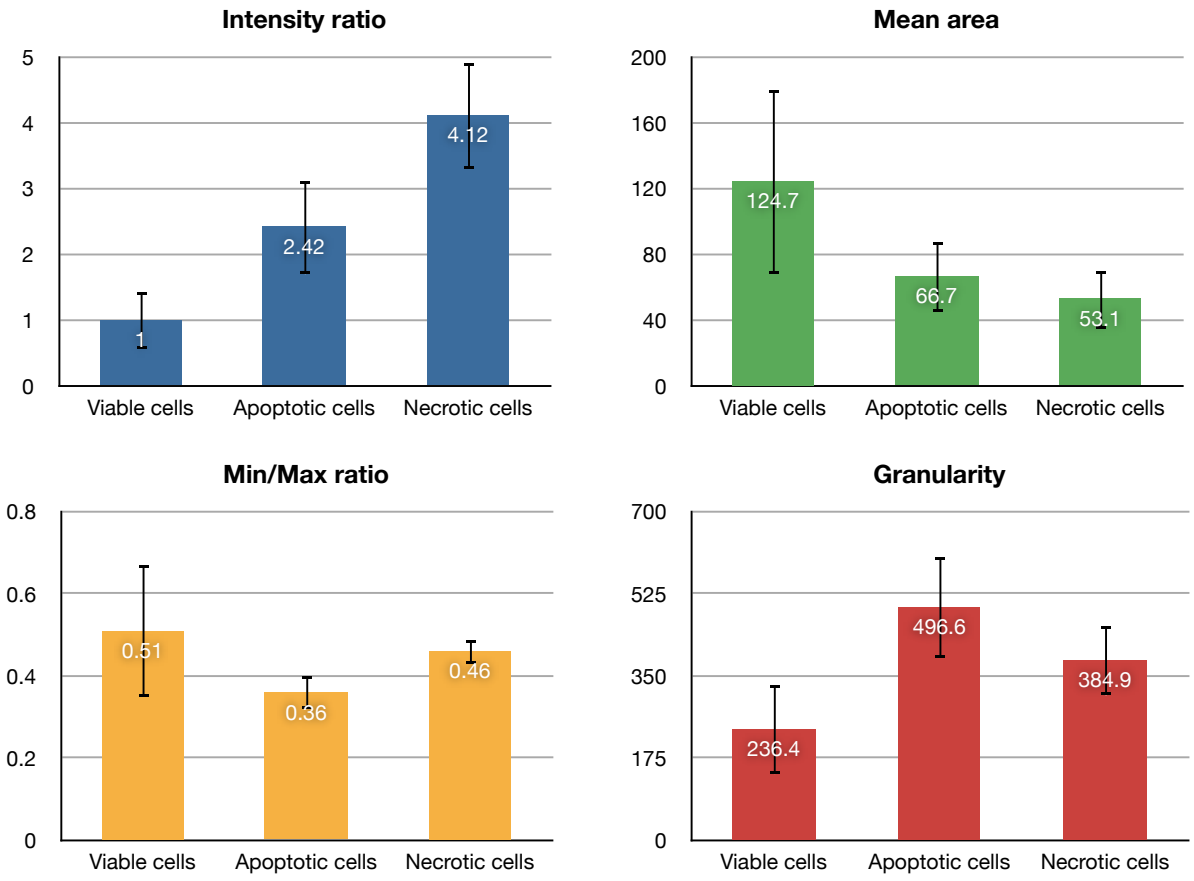

	Intensity ratio		Mean area		Min/Max ratio		Granularity	
	Mean	SD	Mean	SD	Mean	SD	Mean	SD
Viable cells	1	0.43	124.7	56.4	0.51	0.16	236.4	95.1
Apoptotic cells	2.42	0.72	66.7	21.6	0.36	0.04	496.6	107.9
Necrotic cells	4.12	0.82	53.1	18.2	0.46	0.03	384.9	76.1

Figure 17. **Nuclear characterization of different features of viable, apoptotic and necrotic HeLa cells.**

Inter-experimental analysis of nucleus of viable cells, apoptotic cells (confirmed by annexin V conjugate staining) and necrotic cells (confirmed by EthD-1 staining).

- Intensity ratio: ratio between mean viable cells nucleus intensity and apoptotic/necrotic nucleus intensity from the same experiment.
- Mean area: area determined by ROI area after segmentation in μm^2.
- Min/Max ratio: ratio between pixels that have minimum and maximum intensity within ROI after removing the 5^{th} and the 95^{th} percentile of intensity histogram.
- Granularity: average variation between adjacent pixel intensities within a ROI normalized to ROI intensity.

The table below shows the different mean values of the measures and corresponding standard deviations.

Nucleus morphology observed by Hoechst or DAPI staining was changed depending on cell state. Intensity of fluorescence signal in apoptotic cells was by a mean of 2.42 higher than in viable and 4.12 times for necrotic cells. The area of nuclei of apoptotic and necrotic cells was

about two times smaller than viable cells. High variation of viable cell nuclei area could be explained by other cell states that result in lower area like mitosis or by segmentation errors. To minimize these errors, outlier values were removed from analysis as described in Chapter 2.6. Min/Max ratio was not significant although a small effect was observed in apoptotic cells. Granularity reflects intra-nuclear intensity variations and was more pronounced in apoptotic cells certainly due to the nuclear fragmentation process of apoptosis resulting in inhomogeneous nuclear staining.

3.2.3. Live/dead assay

Several experiments of calcein-AM/EthD-1 staining were analyzed. Figure 18 shows intensity ratio for calcein and EthD-1 in dead and living cells. These ratios are reasonably high with around 5 times more intensity of calcein in living cells and 5 times EthD-1 in dead cells. However, z' factor was negative due to high variability of the two probes. The variability of EthD-1 was observable with low signal in cells that had low membrane permeability and very high signal in cells with completely compromised plasma membrane, more advanced in the death process. For calcein, the variability might be due to segmentation method that estimates cytoplasmic area by extension of nucleus and thus the defined cytoplasm ROI might include some background signal in some cells, reducing mean intensity of calcein for those one. Calcein staining was pretty homogeneous from cell to cell but cells that had smaller rounded-shape area (mitotic or early dying cells) showed higher intensity of calcein because of a higher density of calcein in a smaller area.

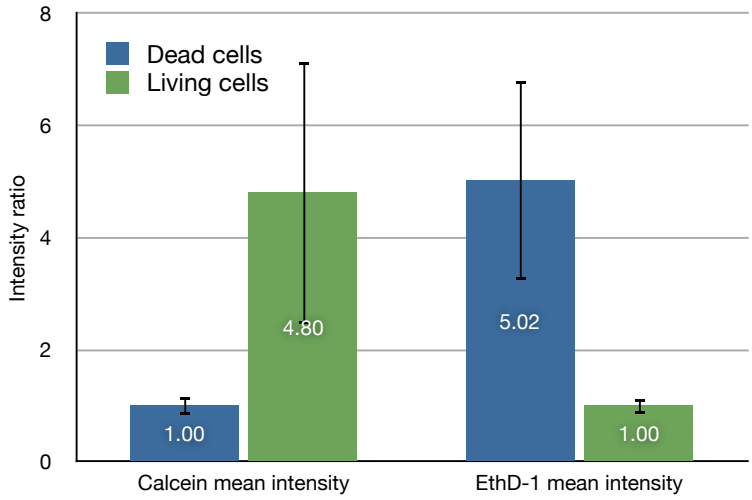

	Calcein mean intensity	SD	EthD-1 mean intensity	SD
Living cells	4.80	2.34	1	0.15
Dead cells	1	0.16	5.02	1.77

Figure 18. **Calcein/EthD-1 mean intensity in viable and dead cells.**

Ratio between mean whole cell intensity of calcein in viable cells and in dead cells (left). Ratio between mean nucleus intensity of EthD-1 in dead cells and in living cells (right). The table below shows numerical values.

The Table 8 shows the different classification of cells in live/dead assay. Living cell event was considered when the object was positive for calcein and negative for Ethd-1. As some dead cells appeared to have residual calcein staining, cells that were calcein (+) and EthD-1 (-) were considered as dead. EthD-1 positive and calcein negative were classified as dead cells as they had compromised membrane and did not have esterase activity. Objects that were negative for calcein and for EthD-1 were set as unknown events and could be segmentation errors.

	EthD-1 (+)	EthD-1 (-)
Calcein (+)	Dead	Viable
Calcein (-)	Dead	Unknown

Table 8. **Cell classification in live/dead assay.**

3.2.4. Annexin V assay

Annexin V conjugate assay aims to detect apoptosis thanks to translocation of phosphatidylserine. An important parameter for this assay is to find a relevant incubation time of apoptosis inducer in order to catch this phenomenon. The Figure 19 shows whole cell normalized intensities of annexin V conjugate in negative control and cells treated with 10^{-5} M staurosporine after different incubation times. A significant difference in signal could be observed after 8h and 24h incubation of staurosporine. However the more the time increase, the higher variability was present. This reflects the heterogeneity of the cell population that have highly variable responses to the stimuli. Discrimination between positive and negative cells was observable after 8h and 24h incubation with one standard deviation separation but z' factor was negative due to high variability of positive control.

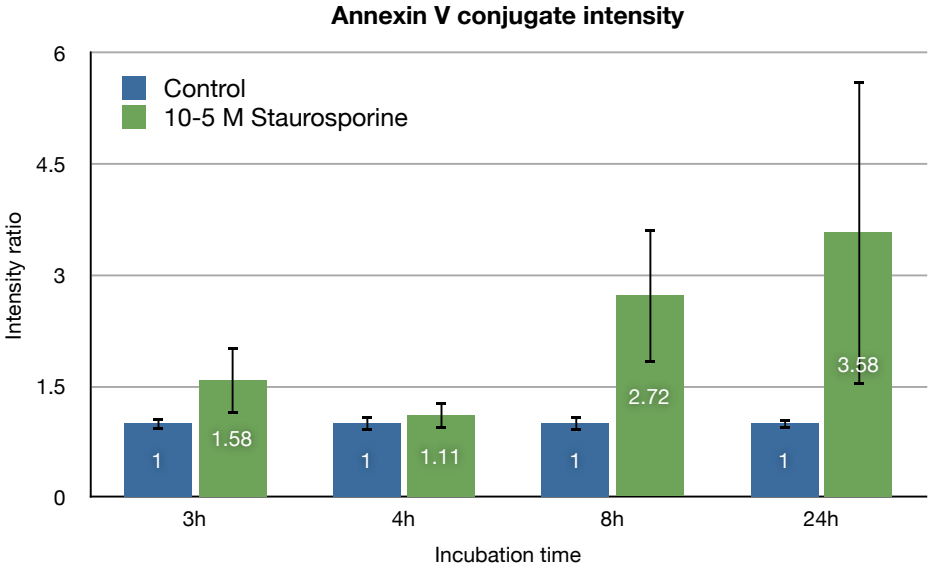

Incubation time	Control	SD	10^{-5} M Staurosporine	SD
3h	1	0.09	1.58	0.46
4h	1	0.11	1.11	0.19
8h	1	0.11	2.72	0.91
24h	1	0.07	3.58	2.06

Figure 19. **Two populations analysis of annexin V conjugate staining.**

Normalized ratio between mean intensity of annexin V conjugate in negative control wells (cells not treated) and mean intensity of cells treated with 10^{-5} M staurosporine after 3h, 4h, 8h and 24h incubation. The table below shows numerical data.

The same data were analyzed by considering three populations (shown in Figure 20): the positive control was divided in the two sub-populations, positive and negative cells for ethidium homodimer-1. The results showed that most of the variability in intensity was due to the EthD-1 positive cells (late apoptotic/necrotic) cells that had more intense staining for annexin V conjugate. As cell membrane is damaged in these cells, annexin V conjugate binds to cytoplasmic-oriented phosphatidylserine and thus gives more signal. Variability in this signal certainly depends on how far cell death process is advanced in each cell. This explain why in Figure 19 the signal after 3h incubation was higher than after 4h, in fact it appeared that the more intense signal at 3h was due to dead cells as shown in Figure 20. EthD-1 negative population showed slightly significant difference in intensity with living cells after 8h and 24h but z' factor was negative for this distribution as well as between viable cells and EthD-1 positive cells because of high variability.

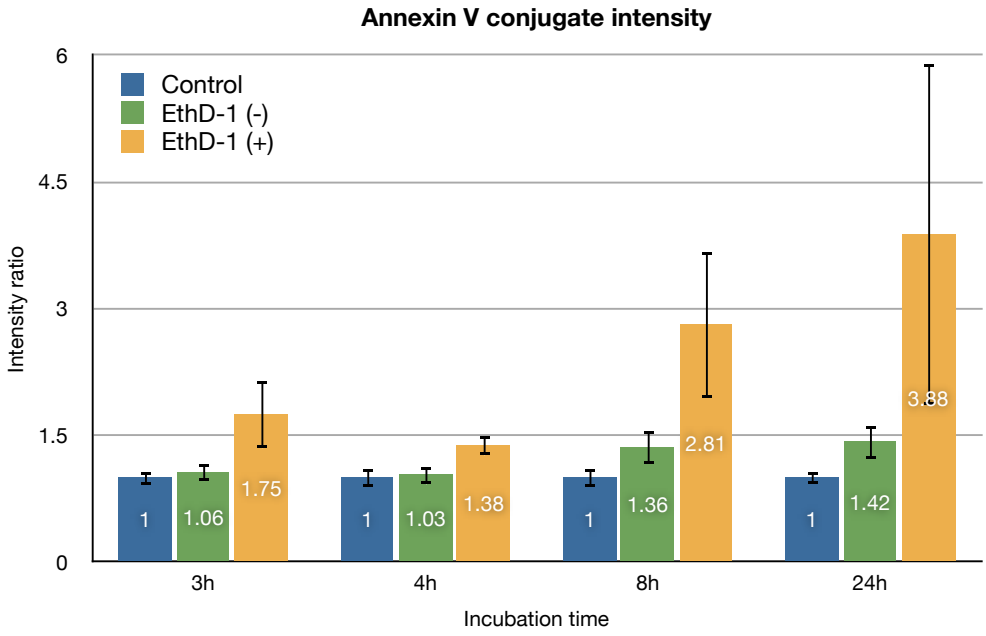

Incubation time	Control	SD	EthD-1 (-)	SD	EthD-1 (+)	SD
3h	1	0.09	1.06	0.10	1.75	0.40
4h	1	0.11	1.03	0.11	1.38	0.12
8h	1	0.11	1.36	0.20	2.81	0.87
24h	1	0.07	1.42	0.20	3.88	2.02

Figure 20. **Three populations analysis of annexin V conjugate staining.**

Normalized ratio between mean intensity of annexin V conjugate in negative control wells (cells not treated) with mean intensity of cells treated with 10^{-5} M staurosporine negative for EthD-1 (green) and positive for EthD-1 (yellow) after 3h, 4h, 8h and 24h incubation. The table below shows numerical data.

Table 9 shows the different populations of cells that could be classified with annexin V assay. Apoptotic event was considered when the object was positive for annexin V and negative for EthD-1 (see Chapter 1.3.5). Annexin (+)/EthD-1 (+) cells were classified as necrotic or late apoptotic cells as they had compromised plasma membrane. When an object was negative for both probes meaning that it had intact membrane and did not show phosphatidylserine translocation, it was set as viable. Unknown events were defined as EthD-1 (+) and annexin V (-) because they showed plasma membrane permeability but no cytoplasmic-side phosphatidylserine staining by annexin V. This contradiction could bring to the conclusion that either cell doesn't have phosphatidylserine in its plasma membrane or this signal is due to aggregate of EthD-1 within a living cell.

	EthD-1 (+)	EthD-1 (-)
Annexin V (+)	Necrotic/Late apoptotic	Apoptotic
Annexin V (-)	Unknown	Viable

Table 9. **Cell classification in annexin V assay.**

In summary, the phosphatidylserine translocation was observable with one standard deviation criteria showing proof of principle of the detection method. The separation between early apoptotic and late apoptotic/necrotic cells was achievable from 8h incubation with 10^{-5} M staurosporine. Nevertheless, the three standard deviations separation required in high throughput screening assays was not reached and the protocol need more optimization to be used in high content assay. In fact, the signal for apoptotic cells was not high enough with the used method. Improvements could be done in segmentation as with current method the signal

is measured in whole cell while annexin V conjugate is located on cell membrane. However, plasmic membrane segmentation was hard due to heterogeneous cell shape. Z stack imaging could increase the whole cell signal by gathering fluorescence emission at different levels so that membrane intensity is averaged in the cytoplasm of the cell but this method would highly increase acquisition time.

3.2.5. LC3B assay

LC3B immunostaining was performed to detect autophagosomes formation in cells treated with 100 µM chloroquine. Image segmentation process is depicted in Figure 21 and exact parameters can be found in Appendix 6.3. This segmentation seemed to efficiently enhance contrast of autophagosomes in cytoplasmic part of cells thanks to different image processing algorithms. As shown in the final mask, autophagosomes (red dots) were present in the cytoplasm of cells treated with chloroquine. In control, some spots were found but were excluded from analysis as they were mainly localized in nucleus part of the cells and sub-objet analyzing was restricted to cytoplasm ROI. This signal could represent nucleolus or noise for some of these spots present in the background.

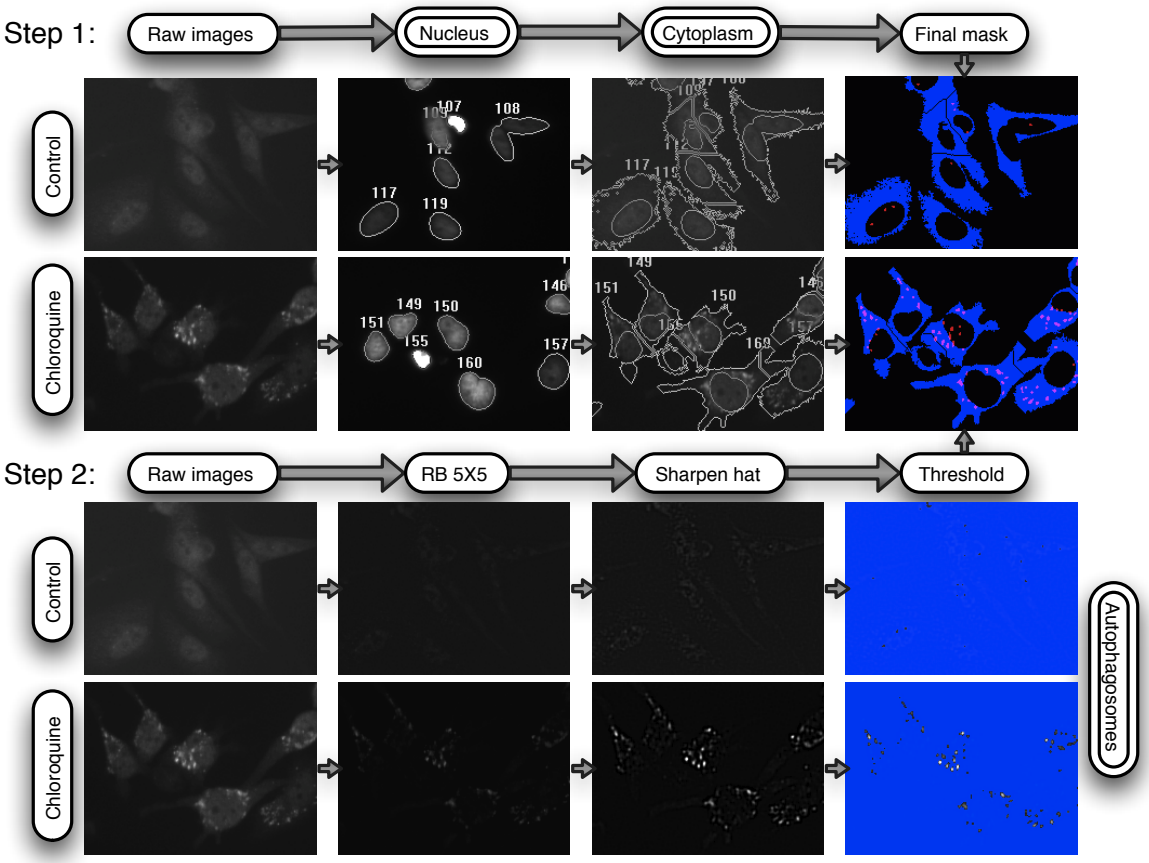

Figure 21. **LC3B immunostaining segmentation process.**

A two-steps segmentation was used to detect autophagosomes in cytoplasm of autophagic cells. The first step defined nucleus with Hoechst staining and cytoplasm thanks to residual fluorescence of immunostaining in this part of the cell. The second step aimed to sharpen autophagosomes in order to discriminate them from cytoplasm fluorescence. RB 5X5 removed cytoplasmic fluorescence and a sharpen hat filter was used to enhance contrast of autophagosomes. The final mask shows detected autophagosomes (red) and cytoplasm mask (blue). Measurements of autophagosomes properties were done only in cytoplasmic part.

Several features were extracted from image segmentation in order to find the most relevant parameter that characterizes autophagic cells. Their comparison in control, cells treated with 50 µM and 100 µM chloroquine for 16h is shown in Figure 22.

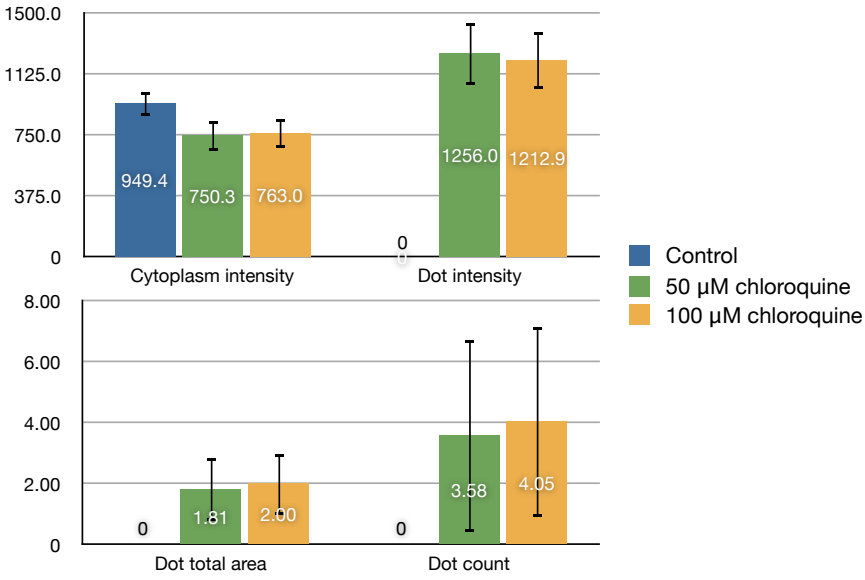

	Control		50 µM chloroquine		100 µM chloroquine	
	Mean	SD	Mean	SD	Mean	SD
Cytoplasm intensity	949.4	77.2	750.3	93.2	763.0	89.3
Dot intensity	0.0	0.0	1'256.0	191.8	1'212.9	173.6
Dot total area	0.00	0.00	1.81	1.03	2.00	1.01
Dot count	0.00	0.00	3.58	3.15	4.05	3.12

Figure 22. **Comparison of features extracted from LC3B staining in control, cells treated with 50 and 100 µM chloroquine.**

Mean cytoplasm intensity, autophagosomes intensity, total area and count extracted from cells stained with 1 µg/ml LC3B antibody and 200X secondary antibody.

Cytoplasmic unspecific staining was slightly higher in control and might be due to higher availability of antibodies as they were not concentrated on autophagosomes. Intensity ratio between mean cytoplasmic intensity and mean dot intensity in autophagic cells was of respectively 1.67 and 1.59 in cells treated with 50 µM and 100 µM chloroquine. With the used segmentation method, the mean number of dot in control was of zero. In cells treated with 50 µM chloroquine, a mean of 3.58 autophagosomes were detected in autophagic cells and this mean was increased to 4.05 autophagosomes in cells treated with 100 µM chloroquine. Nevertheless, this parameter showed high variability with up to 41 autophagosomes detected within a single cell, leading to negative z' factor. Autophagosomes total area in cytoplasm showed similar results as it is closely related to number of autophagosomes. In the same way even with lower variabitity, z' factor was negative.

Observations during segmentation process revealed that cells that appeared dead (round-shaped) had higher uniform cytoplasmic intensity. Segmentation of these cells indicated that high number of autophagosomes were present in these cells. However these detections were only due to the mean higher intensity of the staining and were not dots as they appeared in autophagic cells. Investigation of LC3B immunostaining has to be performed on necrotic and apoptotic cells to get their response to this assay and these observations show that segmentation method is not robust enough to discriminate between the different cellular phenotype that could be present in experiments.

To minimize false positive results, cells that had cytoplasmic intensity higher than three standard deviations apart from the mean intensity were excluded from analysis. The Table 10 show the classification of cell used in LC3B assay.

	Normal cytoplasmic intensity	High cytoplasmic intensity
Presence of autophagosomes	Autophagic	Excluded
Absence of autophagosomes	Viable	Excluded

Table 10. **Cell classification in LC3B assay.**

3.3. *Cell death inducers*

Toxicity of different cell death inducer was determined using alamarBlue® assay with three different protocols (see Chapter 2.2). Dose-response curves were obtained by fitting with GraphPad Prism©. An example for one of the compound (terpinen-4-ol) is given in Figure 23.

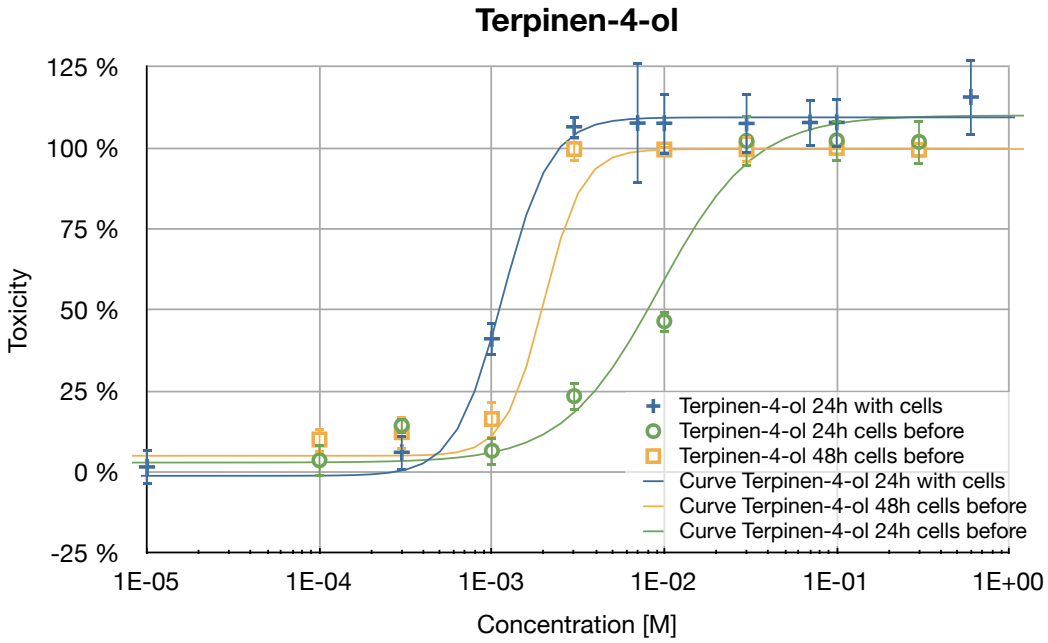

Figure 23. **Toxicity of terpinen-4-ol.**

The figure shows dose-response curves with different protocols for terpinen-4-ol. Curves were fitted with GraphPad Prism©.

Thanks to these curves, IC_{50} (the concentration of compound at which half of the cell population was dead) for each cell death inducer was determined and is shown in Table 11.

Product	IC_{50} [M]		
	Incubated 24h with cells	Incubated 48h cells plated	Incubated 24h cells plated
EDTA	1.0E-03	8.8E-04	1.4E-03
Valproïc acid	6.2E-02	2.0E-03	-
Sodium azide	6.5E-03	5.2E-03	1.7E-02
Terpinen-4-ol	1.2E-03	2.5E-03	6.8E-03
Gambogic acid	1.3E-06	1.7E-06	5.4E-06
Staurosporine	5.4E-07	1.0E-06	1.8E-06
Celastrol	2.5E-06	5.0E-06	1.3E-05
Biozidal	0.1 %	-	-

Table 11. **IC_{50} of different cell death inducers.**

IC_{50} determined with alamarBlue® assay with the different protocols described in Chapter 2.2.

With 24h incubation and cells plated before, valproïc acid did not reach maximal toxicity with the highest concentration used (10^{-1} M, toxicity 26.2%) and curve fitting was thus meaningless. Biozidal, a disinfectant spray used to keep sterility of materials in laminar flow hood, was tested only with 24h incubation added at the same time than the cells in the plate to get an idea of its toxicity. This substance killed all cells at a dilution of only 0.25% volume and could thus induce toxicity if involuntarily diluted with cell medium.

Live/dead assay was performed with these cell death inducers at a concentration close to maximal toxicity. Half of the wells of this plate were analyzed with alamarBlue® assay and results are shown in Table 12.

Product	Concentration [M]	% of viable cells	% of dead cells	% of unknown	Toxicity (Live/Dead assay)	Toxicity (alamarBlue® assay)
Control	**-**	89.2 %	3.3 %	7.4 %	**0 %**	**0 %**
EDTA	**3E-03**	71.4 %	21.3 %	7.3 %	**18.0 %**	**81.6 %**
Valproïc acid	**1E-01**	19.4 %	74.7 %	5.9 %	**71.4 %**	**85.8 %**
Sodium azide	**1E-01**	39.3 %	51.7 %	9.0 %	**48.4 %**	**93.5 %**
Terpinen-4-ol	**3E-02**	8.5 %	82.2 %	9.3 %	**78.8 %**	**95.4 %**
Gambogic acid	**1E-05**	7.0 %	89.0 %	4.0 %	**85.7 %**	**90.0 %**
Staurosporine	**1E-05**	47.6 %	48.2 %	4.2 %	**44.9 %**	**90.8 %**
Celastrol	**3E-05**	1.7 %	94.8 %	3.5 %	**91.4 %**	**92.8 %**

Table 12. **Comparison of live/dead and alamarBlue® assay for different cell death inducers.**

Toxicity of different compounds incubated 24h measured with live/dead assay and alamarBlue® assay on the same plate. Definition of viable cells, dead cells and unknown events are explained in Chapter 3.2.3, Table 8.

Unknown events appended at relatively low rate with a mean of 6.3% for all conditions. As shown in the two last columns of Table 12, high difference of toxicity between live/dead assay and alamarBlue® assay was observed for EDTA, sodium azide and staurosporine. For other compound, toxicity was more or less comparable. This could be explained by the fact that live/dead assay and alamarBlue® assay have different definition of viable cells. In fact, early dying cells could still have reducing power to convert resazurin to resorufin while having only low remaining esterase activity. However, this phenomenon would hardly bring a difference of more than 60% in toxicity (for EDTA) and other factors could have influenced this difference. The various toxic activities of the different compounds (e.g. kinase inhibition for staurosporine or regulation of apoptosis pathway for GBA) that act on different cell pathway could also bring a faster reduction of intracellular esterase activity while keeping reducing environment in the cell. Finally, the compounds could directly interact with the dyes, creating not representative response of the biological system.
Annexin V assay was performed on cell death inducers. An incubation time of the compounds of 6h30 was chosen and results are shown in Table 13.

Product	Concentration [M]	% of necrotic cells	% of apoptic cells	% of unknown	% of viable
Control	**-**	2.2 %	3.5 %	0.7 %	93.6 %
EDTA	**3E-03**	8.4 %	14.5 %	1.5 %	75.6 %
Valproïc acid	**1E-01**	29.1 %	11.6 %	5.8 %	53.4 %
Sodium azide	**1E-01**	16.9 %	39.7 %	3.6 %	39.8 %
Terpinen-4-ol	**3E-02**	10.8 %	4.8 %	39.1 %	45.4 %
Gambogic acid	**1E-05**	13.8 %	12.0 %	5.5 %	68.7 %
Staurosporine	**1E-05**	5.7 %	49.3 %	1.0 %	44.0 %
Celastrol	**3E-05**	45.6 %	3.9 %	8.6 %	41.9 %

Table 13. **Annexin V assay for different cell death inducers.**

Percentage of necrotic, apoptotic and viable cells induced after 6h30 incubation with different compounds. Unknown category is defined in Chapter 3.2.4, Table 9.

Unknown event proportions were low for all compounds except from terpinen-4-ol. In these wells, EthD-1 showed unspecific staining in cells that appeared viable while annexin V staining was inexistent. Thus, these cells were EthD-1 (+)/Annexin V (-) and were classified as unknown events. With high percentage of unknown events, terpinen-4-ol toxicity information might not be reliable.

Incubation time of 6h30 might have been not long enough as only around 50% of cells treated with staurosporine were in apoptotic state and this compound was considered as positive control. An incubation time of 8h could lead to more representative results as described in Chapter 3.1.4. However in these conditions, sodium azide appeared to induce the highest proportion of apoptotic cells after staurosporine. Gambogic acid, a molecule known to induce apoptosis, did not show specific induction of this cell death with an equal proportion of necrotic and apoptotic cells recorded. EDTA triggered slightly more the apoptotic pathway than necrosis. VPA and terpinen-4-ol killed the cells mostly by necrosis with about two times more dying cells by the type of death. Celastrol, an anti-cancer drug known to act as anti-proliferative agent by inducing apoptosis, showed only negligible proportion of apoptotic cells. Especially when compared to control wells, this proportion was lowered to almost zero. This compound induced the highest proportion of necrotic cells. This contradiction could be explained by the fact that the necrotic and the late apoptotic populations are not discriminated in this assay and Celastrol could induce apoptosis in a shorter way than the used incubation time. The apoptotic process might have been more advanced and plasma membrane integrity was already compromised when the assay was performed. Thus, different timeframes and compound concentrations have to be investigated to get reliable information of mechanism leading to cell death.
LC3B immunostaining was used to detect autophagy-inducing compounds. Results are shown in Table 14.

Product	Concentration [M]	% of autophagic cells	% of viable cells	% of excluded
Control	**-**	6.4 %	91.2 %	2.4 %
EDTA	**3E-03**	21.6 %	70.3 %	8.1 %
Valproïc acid	**1E-01**	27.3 %	48.6 %	24.2 %
Sodium azide	**1E-01**	13.1 %	81.5 %	5.4 %
Terpinen-4-ol	**3E-02**	0.0 %	99.1 %	0.9 %
Gambogic acid	**1E-05**	0.2 %	80.7 %	19.1 %
Staurosporine	**1E-05**	9.5 %	81.8 %	8.7 %
Celastrol	**3E-05**	0.4 %	84.8 %	14.8 %
Chloroquine	**1E-04**	59.0 %	40.5 %	0.4 %

Table 14. **LC3B immunostaining of cells treated with different cell death inducers.**

Percentage of autophagic and viable cells induced by 16h incubation with different compounds. Excluded event and cell classification are explained in Chapter 3.2.5, Table 10.

The positive control, chloroquine used at a concentration of 100 μM, induced 59% of autophagic cells with low number of excluded events. In wells treated with terpinen-4-ol, gambogic acid and celastrol, negligible number of autophagic events were recorded. Staurosporine and sodium azide showed relatively low number of autophagosome-containing cells. One fifth of the cells treated with EDTA were engaged in the autophagic process. The compound that induced the most autophagy was VPA and this correlates with information gathered on this substance. However, proportion of excluded events was high for VPA, gambogic acid and celastrol and the robustness of the detection method is discussed in Chapter 3.2.5.

4. Discussion

High content screening is a powerful tool for generating data on fluorescent cell-based assays. In this work, several fluorescent probes for cell viability were tested, optimized and discussed for high content applications. Cell death is a complex mechanism highly regulated by multiple molecules that act on different cell compartments. HCS assays can be multiplexed and have thus great potential to assess cell death mechanisms by reporting different biological activities. In drug discovery, toxicological studies are of high importance as harmful effects of drug candidates have to be well characterized so they can become a treatment.

The importance of liquid handling validation has been highlighted. In fact when working with adherent cells in multiwell plates, dead or dying cells tends to detach from the bottom of the wells and are thus easily removed by liquid aspiration. By removing all or part of the dead cell population, the analyzed sample becomes biased as only living cells are remaining. This effect might be monitored by cell number but high variability is expected in this parameter when working with toxic molecules. Populations homogeneity within single well has also to be taken in account; liquid handling can induce concentration of detached cells in an area of the well. As imaging whole well can produce a consequent volume of data, the part of the well to be imaged has to be chosen judiciously or homogenization has to be performed. If these effects are deeply studied, they might be compensated in data analysis to estimate total toxicity of the compounds. The carelessness of these phenomenons could bring to dramatic erroneous conclusions on the toxicity of the substances tested.

Live/dead assay using calcein/EthD-1 showed significant difference in signal between living and dead cells but high variability. Dual staining was performed on HeLa cells to discriminate the two populations. Residual signal of calcein was observed in dead cells and intensity variations in living cells brought high variability in measured signal. The segmentation method might have contribute to this variation due to inclusion of background signal in the whole cell ROI. Different signal intensities were observed with EthD-1 staining and can depend on how the cell death process is advanced. The information obtained with this assay was compared to alamarBlue® assay on a set of toxic compounds. Significant differences of toxicity were defined by the two assays for some compounds. This result was partly explained by the fact that the two assays target different mechanisms to assess cell viability. AlamarBlue® and calcein/EthD-1 assays both aim to determine viability of a cell population. However, the data obtained with alamarBlue® assay was not less informative than with calcein/EthD-1 staining and this assay might not be optimal solution for live/dead assay in screening. This type of assay is highly informative in tissues or organs staining as spatial distribution of viable and dead cells can be determined. The potential of calcein and EthD-1 staining in high content screening is the multiplexed application in order to determine cell viability while using an assay that tests other cell mechanism. For this purpose, starting conditions have been defined for both probes but further optimized with the multiplexed dye is needed to get lower variability.

Apoptosis detection in HeLa cells was tested with FLICA and annexin V conjugate assay. FLICA staining showed low signal-to-background ratio and separation between positive and negative populations was not achievable. Apoptotic cells were successfully stained with annexin V conjugate assay and significant difference in signal was observed with living cells. This assay allowed to distinguish three cell populations: living cells, early apoptotic cells and necrotic/late apoptotic cells. With this assay, apoptotic cells were detectable only until plasma membrane rupture; after this event, necrotic and apoptotic cells were not separable. High variability was present within control cell population and part of this variation of signal was due to the underlying biological process. In fact, phosphatidylserine translocation appends gradually with loss of flippases activity and therefore the number of available targets for

annexin V on the outer-side of plasma membrane increases with the advancement of the apoptotic process. As apoptosis activation time is not equal for each single cell even under the same experimental conditions, the staining intensity naturally varies upon different cells. An other source of variations between positive cells was segmentation method used. Whole cell measurements were taken and annexin V conjugate is localized on cell membrane. Different toxic compounds were tested with this assay and some substances known to induce apoptosis were negative. This could be explained by the fact that staurosporine was used as control to induce apoptosis and the assay was optimized with this inductor. Other compounds might trigger apoptosis in a different timeframe and show slight variation in the phenotype of apoptotic cells. Annexin V conjugate is a promising assay to detect apoptosis but optimization to minimize variability has to be performed so that this assay reaches screening requirements.
LC3B immunostaining showed an observable difference in phenotypes between control and cells treated with chloroquine. Autophagosomes were detected in the cytoplasm of autophagic cells induced by overnight incubation of 100 mM of chloroquine with a decent signal ratio between autophagosomes and cytoplasm. The developed image analysis method successfully segmented autophagosomes in the cytoplasmic part of autophagic cells while no signal was detected in negative control wells. Segmentation method failed autophagosomes detection in dead cells due to higher cytoplasmic intensity and these cells had to be excluded from analysis. Immunostaining required long and complex protocol with more than 2h30 total incubation times and seven wash steps. This protocol makes LC3B assay difficult to be performed at high throughput and fluorescent conjugated antibody against LC3B would reduce number of steps and incubation times. More, permeabilization of cell membrane was needed to allow antibody to enter the cells. This step made annexin V staining meaningless and cell membrane permeability assessments were no more feasible. Thus if this assay want to be combined with apoptosis detection, annexin V assay has to be acquired before LC3B staining and therefore doubling acquisition time and lengthening protocol. This constraint makes the combined autophagy/apoptosis detection unachievable at high throughput with these assays and compatible only with small set of compounds.
Nucleus analysis showed significant difference in area, intensity and granularity between living, apoptotic and necrotic cells. This information could be used to get insight about cell state if well characterized and compared to appropriate controls. As nuclear stains are present is almost all high content assays to get cell number and position, analysis of nucleus could be a powerful method to get a hint of death mechanism at high throughput and generates no supplementary material costs than the planned assay. Time and resources of image and data analysis would be reasonably increased compared to the importance of the data extracted. This method could typically be used in primary/secondary screen and give a fair estimation of the toxicity of the hits while assessing at the same time their activity on the biological target with the combined assay. Further toxicity studies can then be performed on selected hits with more informative tests on death mechanism. Similarly to nuclear stains, cytoplasmic probes defining cell shape could also give significant information on the viability of the cells with relevant features extracted from image segmentation.
A common question raised by the cell death assays performed was time at which the phenomenon tested append. For instance in annexin V assays, the phosphatidylserine translocation was observable only during a restrict timeframe defined as early apoptosis state. As shown in the different experiments, these timeframes mainly depend on two parameters that are concentration of inducer and incubation time but variability was observed from cell to cell under the same conditions. This means that end-point single condition usually performed in primary/secondary screen is not sufficient to assess toxicity of the compounds tested and would create false negative results. Gradient of concentrations and different time points have to be investigated to precisely determine potential harmful effect of a substance. These

experiments would generate high cost and time at high throughput and are thus suitable only for late state development like hits-to-leads studies. Also, several cellular mechanisms might be tested for the same type of death as different results can be obtained. This is illustrated by the results obtained on the set of toxic compounds where contradictory conclusions on cell viability were drawn using two different assays to get the same data.
Single cell classification was hard as various responses were observed to the different assays. At larger throughput, more phenotypes would be encountered and characterization have to be robust with narrow ranges for positive and negative cells. A multiparametric classification could give better results with less false positive and false negative events thanks to the multiplication of the interval of confidence in which cells are classified. Consequently, an important bottleneck of high content screening assays is the variability of the data due to diversity of living systems.
This work allowed to set up conditions for several fluorescent cell viability probes and conclude about their potential applications in high content screening. The observation and classification of dead or dying cells appeared to be a difficult task at high throughput as cell death is a complex mechanism and needs to be addressed in a thoughtful way. Deeper investigations of the image analysis, data handling and phenotype classification solutions have to be performed to be applicable at large scale.

5. Bibliography

[1] Haney, S. A., LaPan, P., Pan, J. & Zhang, J. High-content screening moves to the front of the line. *Drug Discov Today* **11**, 889-894 (2006).

[2] Zhou, X. & Wong, S. T. High Content Cellular Imaging for Drug Development. *IEEE Sign. Proc. Mag.* **23**, 170-174 (2006).

[3] Comley, J. High content screening: emerging importance of novel reagents/probes and pathway analysis. *Drug Discovery World*, 31-53 (2005).

[4] Zingler, K. & Heyse, S. High content screening – the next challenge: effective data mining and exploration. *Drug Discovery World*, 27-34 (2008).

[5] Krausz, E. High-content siRNA screening. *Mol Biosyst* **3**, 232-240, doi:10.1039/b616187c (2007).

[6] Eisenberg-Lerner, A., Bialik, S., Simon, H. U. & Kimchi, A. Life and death partners: apoptosis, autophagy and the cross-talk between them. *Cell Death Differ* **16**, 966-975 (2009).

[7] Los, M. *et al.* Activation and caspase-mediated inhibition of PARP: a molecular switch between fibroblast necrosis and apoptosis in death receptor signaling. *Mol Biol Cell* **13**, 978-988 (2002).

[8] Yousefi, S. *et al.* Calpain-mediated cleavage of Atg5 switches autophagy to apoptosis. *Nat Cell Biol* **8**, 1124-1132 (2006).

[9] Cotter, T. G. Apoptosis and cancer: the genesis of a research field. *Nat Rev Cancer* **9**, 501-507 (2009).

[10] Hotchkiss, R. S., Strasser, A., McDunn, J. E. & Swanson, P. E. Cell death. *N Engl J Med* **361**, 1570-1583 (2009).

[11] Thornberry, N. A. & Lazebnik, Y. Caspases: enemies within. *Science* **281**, 1312-1316 (1998).

[12] van Engeland, M., Nieland, L. J., Ramaekers, F. C., Schutte, B. & Reutelingsperger, C. P. Annexin V-affinity assay: a review on an apoptosis detection system based on phosphatidylserine exposure. *Cytometry* **31**, 1-9 (1998).

[13] Mizushima, N. Autophagy: process and function. *Genes Dev* **21**, 2861-2873 (2007).

[14] Takeshige, K., Baba, M., Tsuboi, S., Noda, T. & Ohsumi, Y. Autophagy in yeast demonstrated with proteinase-deficient mutants and conditions for its induction. *J Cell Biol* **119**, 301-311 (1992).

[15] Mortimore, G. E. & Poso, A. R. Intracellular protein catabolism and its control during nutrient deprivation and supply. *Annu Rev Nutr* **7**, 539-564 (1987).

[16] He, H. *et al.* Post-translational modifications of three members of the human MAP1LC3 family and detection of a novel type of modification for MAP1LC3B. *J Biol Chem* **278**, 29278-29287 (2003).

[17] Marino, G. & Lopez-Otin, C. Autophagy: molecular mechanisms, physiological functions and relevance in human pathology. *Cell Mol Life Sci* **61**, 1439-1454 (2004).

[18] Golstein, P. & Kroemer, G. Cell death by necrosis: towards a molecular definition. *Trends Biochem Sci* **32**, 37-43 (2007).

[19] Johnson, I. Fluorescent probes for living cells. *Histochem J* **30**, 123-140 (1998).

[20] Kubista, M., Akerman, B. & Norden, B. Characterization of interaction between DNA and 4',6-diamidino-2-phenylindole by optical spectroscopy. *Biochemistry* **26**, 4545-4553 (1987).

[21] Bratosin, D., Mitrofan, L., Palii, C., Estaquier, J. & Montreuil, J. Novel fluorescence assay using calcein-AM for the determination of human erythrocyte viability and aging. *Cytometry A* **66**, 78-84 (2005).

[22] Homolya, L. *et al.* Fluorescent cellular indicators are extruded by the multidrug resistance protein. *J Biol Chem* **268**, 21493-21496 (1993).

[23] Petronilli, V. *et al.* Transient and long-lasting openings of the mitochondrial permeability transition pore can be monitored directly in intact cells by changes in mitochondrial calcein fluorescence. *Biophys J* **76**, 725-734 (1999).

[24] Reutelingsperger, C. P., Hornstra, G. & Hemker, H. C. Isolation and partial purification of a novel anticoagulant from arteries of human umbilical cord. *Eur J Biochem* **151**, 625-629 (1985).

[25] Raynal, P. & Pollard, H. B. Annexins: the problem of assessing the biological role for a gene family of multifunctional calcium- and phospholipid-binding proteins. *Biochim Biophys Acta* **1197**, 63-93, doi:0304-4157(94)90019-1 [pii] (1994).

[26] Bickle, M. High-content screening: a new primary screening tool? *IDrugs* **11**, 822-826 (2008).

[27] Zhang, J. H., Chung, T. D. & Oldenburg, K. R. A Simple Statistical Parameter for Use in Evaluation and Validation of High Throughput Screening Assays. *J Biomol Screen* **4**, 67-73 (1999).

[28] Niederlein, A., Meyenhofer, F., White, D. & Bickle, M. Image analysis in high-content screening. *Comb Chem High Throughput Screen* **12**, 899-907, doi:CCHTS-23 [pii] (2009).

[29] Beucher, S. & Lantuejoul, C. in *International Workshop on Image Processing: Real-time Edge and Motion Detection/Estimation, Rennes, France.*

6. Appendices

6.1. Cell death inducers

The following sheets describe different products used to induce cell death in HeLa cells.

- EDTA
- Gambogic acid
- Sodium azide
- Staurosporine
- Terpinen-4-ol
- Valproïc acid

Product information sheet : EDTA

Name: Ethylenediaminetetraacetic acid (EDTA)

Information: Chelating agent. Used in cell culture to bind calcium ions and prevent cadherins interactions, thus facilitating detachment of adherent cells.

Chemical formula: $C_{10}H_{16}N_2O_8$

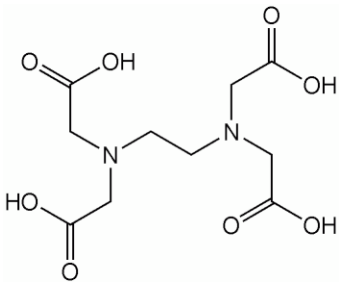

EDTA chemical structure.

Molecular weight: 292.24 g mol^{-1}

Solubility: 10^{-1} M in H_2O

Toxicity data: Toxicity according to 3 protocols:

- 24h incubation added with the cells
- 24h incubation added 24h after plating cells
- 48h incubation added 24h after plating cells

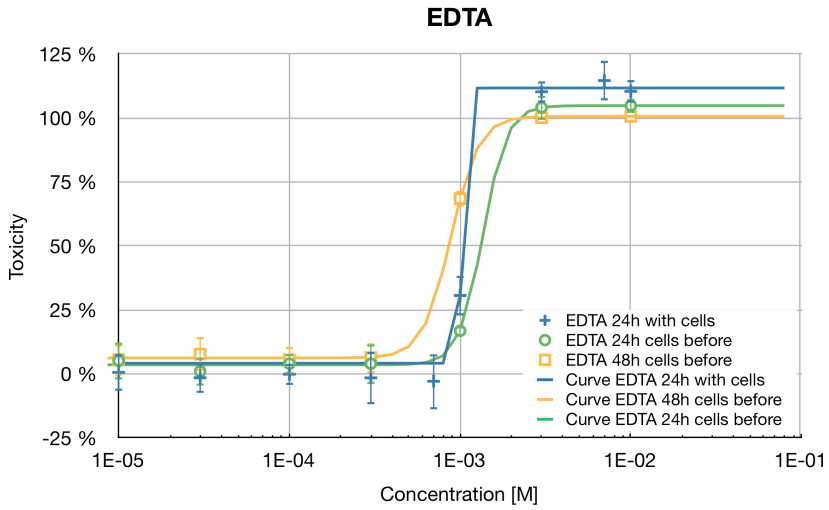

	EDTA 24h with cells	EDTA 48h cells before	EDTA 24h cells before
EC_{50}	1.03E-03	8.83E-04	1.36E-03

Product information sheet : Gambogic acid

Name: Gambogic acid

Information: Natural product isolated from the resin of plants *Garcinia* species. Known to induce apoptosis by upregulating Bax and inhibiting anti-apoptotic Bcl-2 proteins expression.

Chemical formula: $C_{38}H_{44}O_8$

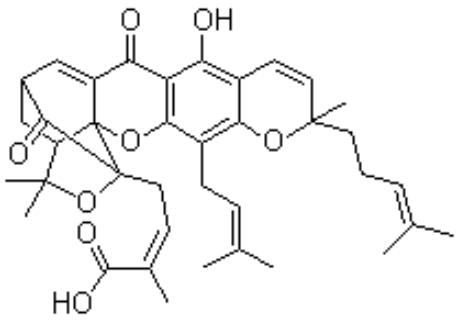

Gambogic acid chemical structure

Molecular weight: 628.8 g mol^{-1}

Solubility: 10^{-2} M in DMSO

Toxicity data: Toxicity according to 3 protocols:

- 24h incubation added with the cells
- 24h incubation added 24h after plating cells
- 48h incubation added 24h after plating cells

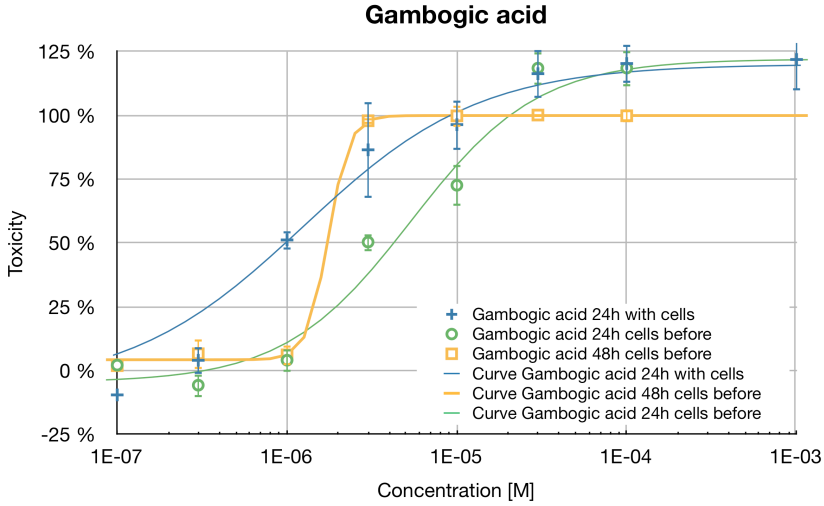

	GBA 24h with cells	GBA 48h cells before	GBA 24h cells before
EC_{50}	1.25E-06	1.75E-06	5.38E-06

Product information sheet : Sodium azide

Name: Sodium azide

Information: Inhibits cytochrome oxydase by binding to the heme factor. It is very toxic, mutagen and preservative.

Chemical formula: NaN_3

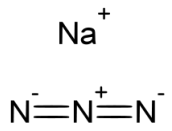

Sodium azide chemical structure

Molecular weight: 65.0099 g mol^{-1}

Solubility: 6.4 M in H_2O
$5 \cdot 10^{-2}$ in alcohol

Toxicity data: Toxicity according to 3 protocols:

- 24h incubation added with the cells
- 24h incubation added 24h after plating cells
- 48h incubation added 24h after plating cells

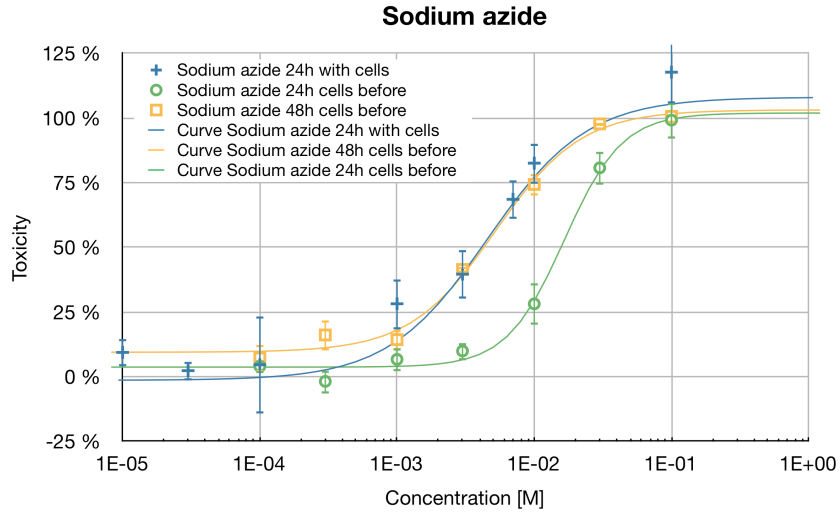

	NaN_3 24h with cells	NaN_3 48h cells before	NaN_3 24h cells before
EC_{50}	4.57E-03	5.21E-03	1.66E-02

Product information sheet : Staurosporine

Name: Staurosporine

Information: Natural product isolated from bacterium *Streptomyces staurosporeus*, this protein is inhibiting protein kinases by preventing ATP from binding to them. It is known to induce apoptosis.

Chemical formula: $C_{28}H_{26}N_4O_3$

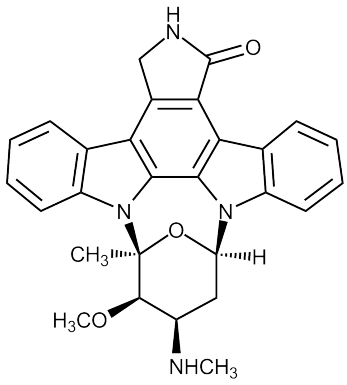

Staurosporine chemical structure

Molecular weight: 466.53 g mol^{-1}

Solubility: 10^{-2} M in DMSO

Toxicity data: Toxicity according to 3 protocols:

- 24h incubation added with the cells
- 24h incubation added 24h after plating cells
- 48h incubation added 24h after plating cells

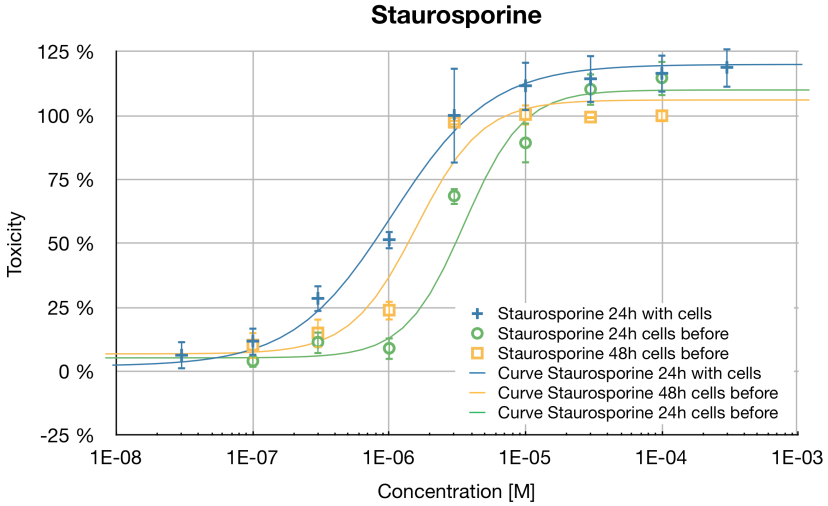

	Stauro 24h with cells	Stauro 48h cells before	Stauro 24h cells before
EC_{50}	1.05E-06	1.58E-06	3.55E-06

Product information sheet : Terpinen-4-ol

Name: Terpinen-4-ol

Information: Natural product isolated from tea tree oil, an oil derived from an Australian plant *Melaleuca alternifolia*. It is used for its anti-microbial, anti-inflammatory and anti-cancer effect although its mechanism of action is not well known.

Chemical formula: $C_{10}H_{18}O$

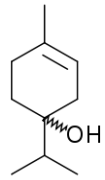

Terpinen-4-ol chemical structure

Molecular weight: 154.25 g mol^{-1}

Solubility: 3 10^{-3} M in H_2O

Toxicity data: Toxicity according to 3 protocols:

- 24h incubation added with the cells
- 24h incubation added 24h after plating cells
- 48h incubation added 24h after plating cells

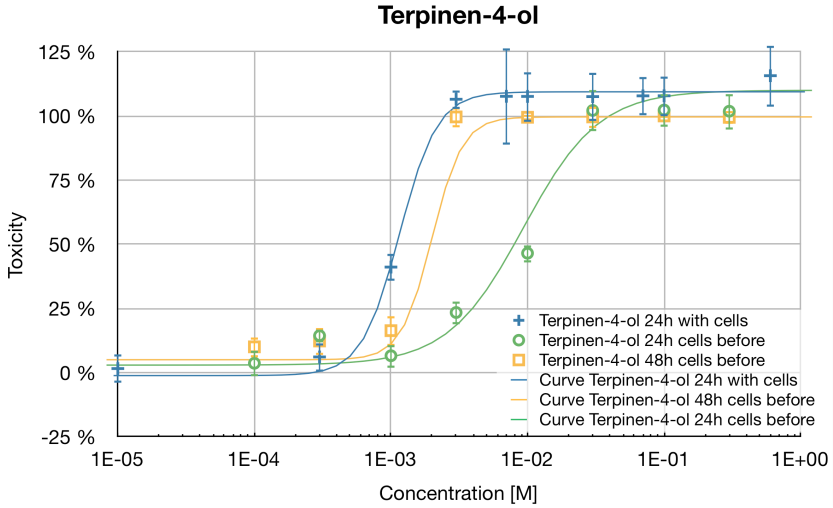

	T4O 24h with cells	T4O 48h cells before	T4O 24h cells before
EC_{50}	1.16E-03	2.00E-03	9.33E-03

Product information sheet : Valproïc acid

Name: Valproïc acid

Information: Inhibitor of histone deacetylase and used as anticonvulsant and mood-stabilizing drug. It has been shown to induce autophagy.

Chemical formula: $C_8H_{12}O_2$

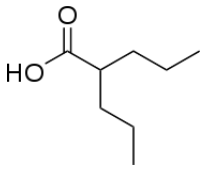

Valproïc acid chemical structure

Molecular weight: 144.21 g mol^{-1}

Solubility: 1 M in H_2O

Toxicity data: Toxicity according to 3 protocols:

- 24h incubation added with the cells
- 24h incubation added 24h after plating cells
- 48h incubation added 24h after plating cells

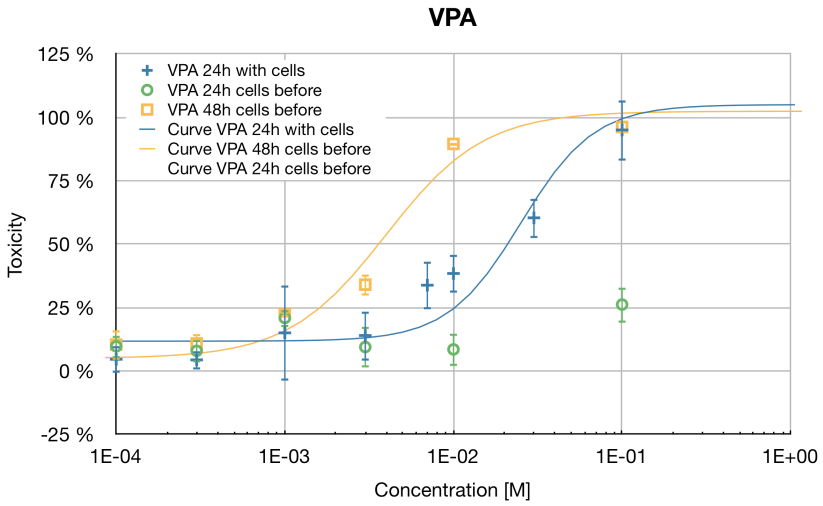

	VPA 24h with cells	VPA 48h cells before	VPA 24h cells before
EC_{50}	2.51E-02	3.98E-03	-

6.2. Staining protocols

Hoechst

0. At J-1, plate 3'000 HeLa cells per well.
1. Add Hoechst 33342 staining solution as 10X concentrated for a final concentration of 1 μg/ml. A 1X concentrated solution could also be used after removing cell medium.
2. Incubate at 37°C for minimum 15 min or at RT for 30 min.

DAPI

0. At J-1, plate 3'000 HeLa cells per well.
1. Add DAPI staining solution as 10X concentrated for a final concentration of 10 μg/ml. A 1X concentrated solution could also be used after removing cell medium.
2. Incubate at 37°C for minimum 15 min or at RT for 30 min.
3. Wash 1X with 100 μl PBS per well.

Calcein

0. At J-1, plate 3'000 HeLa cells per well.
1. Add calcein staining solution as 10X concentrated for a final concentration of 0.5 μg/ml. A 1X concentrated solution could also be used after removing cell medium.
2. Incubate at 37°C for 30 min or at RT for 45 min.
3. (Optional) Wash 1X with 100 μl PBS per well gives better results.

Ethidium homodimer-1

0. At J-1, plate 3'000 HeLa cells per well.
1. Add EthD-1 staining solution as 10X concentrated for a final concentration of 1 μM. A 1X concentrated solution could also be used after removing cell medium.
2. Incubate at 37°C for 30 min or at RT for 50 min.

DAPI, calcein and EthD-1

0. At J-2, plate 3'000 HeLa cells per well.
1. At J-1, treat control wells with 10 mM $CuSO_4$ added as 10X concentrated solution.
2. Add staining solution as 10X concentrated for final concentration of 0.5 μg/ml calcein, 10 μg/ml DAPI and 1 μM EthD-1.
3. Incubate at 37°C for 30 min or at RT for 50 min.
4. Wash 1X with 100 μl PBS per well.

Annexin V conjugate

0. At J-2, plate 3'000 HeLa cells per well.
1. At J-1, treat control wells with 10 μM staurosporine added as 10X concentrated solution.
2. Wash 1X with 100 μl PBS per well.
3. Add 90 μl of annexin-binding buffer (10 mM HEPES, 140 mM NaCl, 2.5 mM $CaCl_2$) per well.
4. Add 10 μl of staining solution containing 5X annexin V conjugate stock solution, 10 μg/ml Hoechst 33342 and 10 μM EthD-1 (final well concentration 50X annexin V conjugate, 1 μg/ml Hoechst 33342 and 1 μM EthD-1).
5. Incubate at RT for 30 min.

6. (Optional) Wash 1X with annexin-binding buffer.

LC3B immunostaining

0. At J-2, plate 3'000 HeLa cells per well.
1. At J-1, treat control wells with 100 mM chloroquine added as 10X concentrated solution.
2. Fix with 3.7% PFA by removing medium and adding 50 µl PFA per well and incubating at RT for 15 min.
3. Wash 3X with 100 µl PBS per well.
4. Permeabilize cell membrane with 0.2% Triton X-100 by removing PBS and adding 50 µl Triton X-100 per well and incubating at RT for 15 min.
5. Remove Triton X-100 solution and add primary rabbit anti-LC3B antibody at a concentration of 1 µg/ml as 50 µl per well.
6. Incubate 1h at RT.
7. Wash 3X with 100 µl PBS per well.
8. Remove PBS solution and add 200X secondary goat anti-rabbit antibody as 50 µl per well.
9. Incubate 1h at RT.
10. Wash 1X with 100 µl PBS per well.
11. Remove PBS solution and add 1 µg/ml Hoechst 33342 solution as 50 µl per well.
12. Incubate 15 min at RT.

6.3. Segmentation parameters

Segmentation parameters used with Attovision™.

Whole cell/nucleus segmentation

Processing tab:

Flat field correction – on
Select dyes and assign corresponding lamp
Background subtraction - off

Segmentation tab:

Number of steps: 2
Step 1:
Re-segment
Use system ROIs: Polygon
Channel A: choose nuclear probe (Hoechst/DAPI)
Segmentation setup:
Shape: Polygon
Image Pre-processing: RB 25X25, Shading
Threshold: Automatic, levels: 1
Split: Watershed, Erosion Factor: 4
Scrap: Min: 50, Max: 2000
Options: Dilatation Width: 9
ROIs: Whole cell
Step 2:
Same as Step 1 except from:
Options: Dilatation Width: 0
ROIs: Nucleus

Dye Thresholds tab:

-

Measure tab:

For whole cell probes, select features to extract.
For nucleus probes, select Sub Object. Choose corresponding image and select ROIs: Nucleus. Choose analysis output.

LC3B assay segmentation

Processing tab:

Flat field correction – on
Select dyes and assign corresponding lamp
Background subtraction - off

Segmentation tab:

Number of steps: 2
Step 1:
Re-segment
Use system ROIs: Cyto-dual
Channel A: choose nuclear probe (Hoechst/DAPI)

Channel B: Choose LC3B probe (Alexa 647)
Segmentation setup:
Shape: Dual channel (Exclude Center)
Tab A:
Image Pre-processing: RB 25X25, Shading
Threshold: Automatic, levels: 1
Split: Watershed, Erosion Factor: 4
Scrap: Min: 50, Max: 2000
Options: Dilatation Width: 0
Tab B:
Image Pre-processing: RB 25X25
Threshold: Automatic, levels: 1
Split: Watershed, Erosion Factor: 4
Scrap: Min: 50, Max: 5000
Options: Dilatation Width: 50
ROIs: Cytoplasm

Step 2:
Re-segment
Use system ROIs: Polygon
Channel A: choose LC3B probe (Alexa 647)
Segmentation setup:
Shape: Polygon
Image Pre-processing: RB 5X5, Sharpen Hat
Threshold: Automatic, levels: 1 + 6-8%
Split: Watershed, Erosion Factor: 2
Scrap: Min: 2, Max: 25
Options: Dilatation Width: 0
ROIs: No ROI

Dye Thresholds tab:
-

Measure tab:
Select Sub Object for LC3B probe (Alexa 647). Choose corresponding image (LC3B image) and select ROIs: No ROI. Choose analysis output.

6.4. VBA Macro information

These macros reformat outputs of experiments in 96-well analyzed with Attovision™ and put all images in a single folder. They are compatible with Microsoft® Office Excel 2004 on Windows environment. They won't work with later version of this software, as VBA language is no more supported.
To start, open Excel file containing the macros (BSF_HCA_Macro.xls). Then, choose between "Reformat output" or "Extract images".

Reformat output

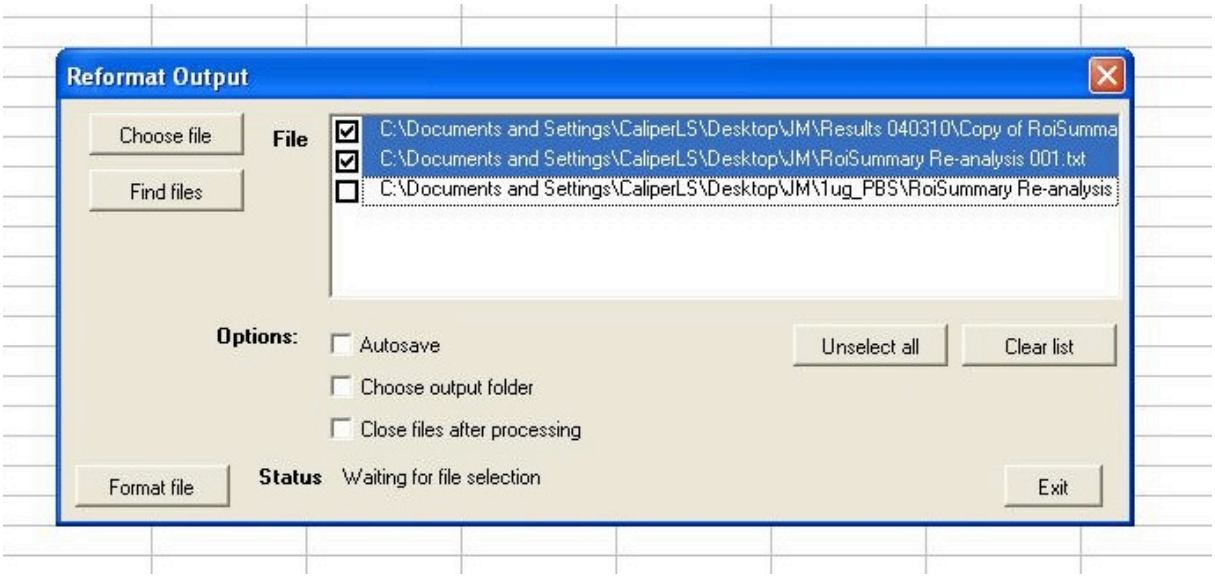

1. Choose the files to analyze by either click on "Choose file" button to select single file (e.g. RoiSummary Re-analysis 001) or use "Find files" to enter a keyword (e.g. Re-analysis) and find all files containing this keyword in a parent folder. The second option is useful when several acquisitions or analysis were performed.
2. Tip the files to reformat in the obtained list. Note "Unselect all" and "Clear list" buttons.
3. Choose options. "Autosave" will automatically save the reformatted file with the name of the parent folder. If not selected, a filename will be asked after reformatting. "Choose output folder" option let you save all reformatted files in a single folder. If not selected, the saving path will be asked for each reformatted files. "Close files after processing" will automatically close Excel sheet containing reformatted output.
4. Format files. Check that you tipped the files to reformat and different options and click "Format file" button. If selected, enter the information for saving the files. "Status" indicates which file is being processed and when the reformatting is finished.

Notes: Excel sheet limit might be reached (256 columns and 65'536 rows). In this case reformatting will be stopped and a warning will appear. To finish reformatting, duplicate the analysis file and open it with a text editor. Delete the reformatted part until the beginning of the last well reformatted (starting with date and time of acquisition) and run the macro on this file.

Extract images

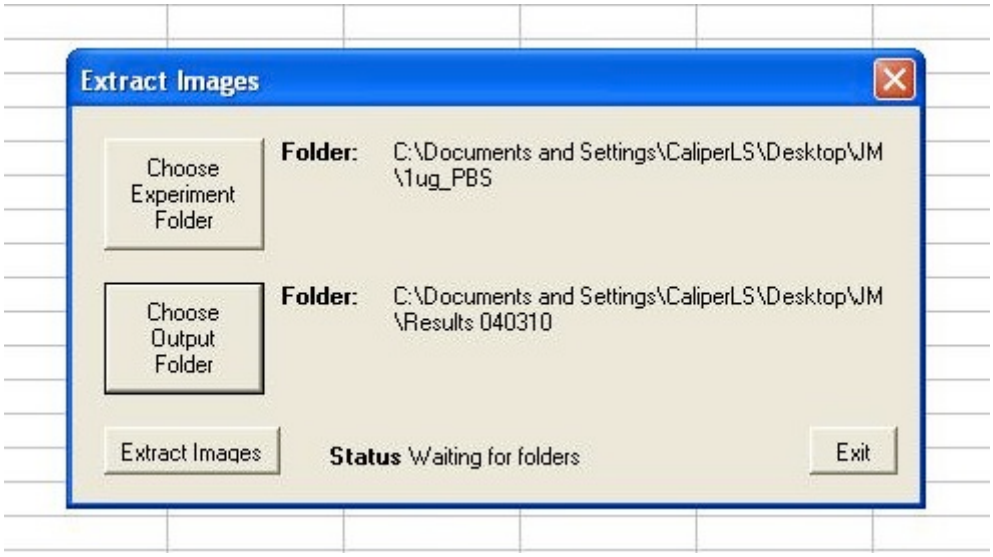

1. Choose experiment folder. Click “Choose Experiment Folder” button to select the folder containing all files of your experiment (e.g. 2010-04-21_000).
2. Choose output folder. Click “Choose Output Folder” button to select or create the folder in which all found images will be copied.
3. Extract images. Click “Extract Images” to find all TIF images contained in the experiment folder and copy them in the output folder. “Status” indicates when the process is finished.